Integrated soybean transcriptomics, metabolomics, and chemical genomics reveal the importance of the phenylpropanoid pathway and antifungal activity in resistance to the broad host range pathogen *Sclerotinia sclerotiorum*.

Ashish Ranjan[1], Nathaniel M. Westrick[1], Sachin Jain[1], Jeff S. Piotrowski[2#], Manish Ranjan[3], Ryan Kessens[1], Logan Stiegman[1], Craig R. Grau[1], Damon L. Smith[1], and Mehdi Kabbage[1]*

[1]Department of Plant Pathology, University of Wisconsin-Madison, Madison, WI, USA

[2]The Great Lakes Bioenergy Research Center, University of Wisconsin-Madison, Madison, WI, USA

[3]School of Computational and Integrative Sciences, Jawaharlal Nehru University, New Delhi, India

[#]Current affiliation: Yumanity Therapeutics, Cambridge, MA, USA

*To whom correspondence should be addressed: kabbage@wisc.edu

ABSTRACT

Sclerotinia sclerotiorum, a predominately necrotrophic fungal pathogen with a broad host range, causes a significant yield limiting disease of soybean called Sclerotinia stem rot (SSR). Resistance mechanisms against SSR are poorly understood, thus hindering the commercial deployment of SSR resistant varieties. We used a multiomic approach utilizing RNA-sequencing, Gas chromatography-mass spectrometry-based metabolomics and chemical genomics in yeast to decipher the molecular mechanisms governing resistance to *S. sclerotiorum* in soybean. Transcripts and metabolites of two soybean recombinant inbred lines, one resistant, and one susceptible to *S. sclerotiorum* were analyzed in a time course experiment. The combined results show that resistance to *S. sclerotiorum* in soybean is associated in part with an early accumulation of JA-Ile ((+)-7-iso-Jasmonoyl-L-isoleucine), a bioactive jasmonate, increased ability to scavenge reactive oxygen species (ROS), and importantly, a reprogramming of the phenylpropanoid pathway leading to increased antifungal activities. Indeed, we noted that phenylpropanoid pathway intermediates such as, 4-hydroxybenzoate, ferulic acid and caffeic acid were highly accumulated in the resistant line. *In vitro* assays show that these metabolites and total stem extracts from the resistant line clearly affect *S. sclerotiorum* growth and development. Using chemical genomics in yeast, we further show that this antifungal activity targets ergosterol biosynthesis in the fungus, by disrupting enzymes involved in lipid and sterol biosynthesis. Overall, our results are consistent with a model where resistance to *S. sclerotiorum* in soybean coincides with an early recognition of the pathogen, leading to the modulation of the redox capacity of the host and the production of antifungal metabolites.

AUTHOR SUMMARY

Resistance to plant fungal pathogens with predominately necrotrophic lifestyles is poorly understood. In this study, we use *Sclerotinia sclerotiorum* and soybean as a model system to identify key resistance components in this crop plant. We employed a variety of omics approaches in combination with functional studies to identify plant processes associated with resistance to *S. sclerotiorum*. Our results suggest that resistance to this pathogen is associated in part with an earlier induction of jasmonate signaling, increased ability to scavenge reactive oxygen species, and importantly, a reprogramming of the phenylpropanoid pathway resulting in increased antifungal activities. These findings provide specific plant targets that can exploited to confer resistance to *S. sclerotiorum* and potentially other pathogens with similar lifestyle.

INTRODUCTION

Sclerotinia sclerotiorum (Lib.) de Bary, is a plant fungal pathogen with a predominately necrotrophic lifestyle and worldwide distribution that is known to infect over 400 plant species (1). On soybean (*Glycine max* (L.) Merr.), it causes sclerotinia stem rot (SSR), a significant and challenging yield limiting disease. Data suggest that 1.6 billion kilograms of soybean are lost each year to SSR in the US alone, making it the second most damaging disease of soybean (2,3). Globally, SSR can cause yield reductions as high as 60% (4). Soybeans are an important source of plant proteins and oils globally (5–7), these products can also be significantly affected by SSR (8). Management strategies against SSR rely largely on chemical control (9), though cultural practices such as crop rotation, seeding rate and row spacing modifications have been used with limited success (3). While genetic resistance is by far more sustainable, our understanding of resistance mechanisms against this pathogen is limited, and current commercial varieties lack adequate levels of resistance to SSR.

In the past two decades, studies have increased our understanding of *S. sclerotiorum* pathogenic development. *S. sclerotiorum* is a prolific producer of cell wall degrading enzymes (CWDEs) that contribute to its pathogenic success (10). In addition to its lytic repertoire, the pathogenic success of *S. sclerotiorum* relies on the key virulence factor oxalic acid (OA). Mutants that are defective in OA production are weakly pathogenic (11–14). OA was proposed to contribute to pathogenesis by acidifying host tissues and sequestering calcium from host cell walls, facilitating the action of CWDEs. However, recent studies showed that *S. sclerotiorum* relies on OA to induce programmed cell death (PCD) in the host to its own benefit (11,15). OA induced PCD is dependent on the production of reactive oxygen species (ROS) in the plant (14,15). This

78 points to the importance of the ROS machinery in the pathogenic success of this pathogen. Indeed,
79 we showed that *S. sclerotiorum*, via OA, co-opts soybean NADPH oxidases to increase host ROS,
80 and that the silencing of specific NADPH oxidases confers enhanced resistance to this fungus (16).
81 In the addition to OA, other virulence factors targeting host responses are known to contribute to
82 the pathogenicity of *S. sclerotiorum*. The necrosis and ethylene-inducing like proteins (NLPs)
83 SsNEP1 and SsNEP2 induce cell death in tobacco leaves, thus contributing to disease
84 establishment (17). The secreted chorismate mutase (SsCM1) and integrin-like protein (SsITL)
85 were proposed to target Arabidopsis defenses by affecting salycilic acid and jasmonate signaling,
86 respectively (18,19). The ability of *S. sclerotiorum* to detoxify plant chemical defenses has also
87 been discussed (20). Unfortunately, these studies have largely focused on the fungal side of this
88 interaction, and only provide glimpses into the plant mechanisms governing resistance to this
89 pathogen, mainly in model plants. In soybean, Bi-parental linkage mapping led to the discovery of
90 many quantitative trait loci (QTL) for resistance to this pathogen. Remarkably, a total of 103 QTL
91 on 18 of the 20 soybean chromosomes have been recorded in SoyBase (21) with minimal overlap
92 between QTL reported by different studies (9,22–26). Despite these efforts, gene level and
93 mechanistic details of soybean resistance mechanisms against *S. sclerotiorum* remain unknown.
94 Recent advances in Next-Generation RNA sequencing (RNAseq) allow for cost-efficient
95 and powerful examination of global differences in the transcriptional response to environmental
96 cues. The application of RNAseq approaches in soybean-*S. sclerotiorum* interaction studies will,
97 most assuredly, contribute to the development of molecular genetic resources crucial for
98 mechanistic and translational research. Transcriptomics were used to study the interaction of *S.*
99 *sclerotiorum* with other non-model plant hosts, including canola (27–29), pea (30), and common
100 bean (31). While informative, these studies were solely based on gene expression comparisons,

and thus may not provide a complete picture of the flow of biologic information. When coupled with other omics approaches, such as metabolomics and chemical genomics, RNAseq can provide a much greater understanding of the biology, by integrating genetic responses of a particular interaction to functional consequences. Herein, we apply multi-omics approaches to identify and validate resistance processes against *S. scleoriorum* in soybean lines generated in our breeding program. The identification of these processes will not only increase our understanding of the soybean-*S. sclerotiorum* interaction but will also facilitate the introgression of resistance into soybean varieties.

Our recent breeding efforts led to the identification of several recombinant inbred lines (RILs) highly resistant to *S. sclerotiorum* (9), using the soybean line W04-1002 as the main source of resistance (32). After multiple generations of greenhouse selection, we have chosen two RILs originating from the same cross; one resistant (91-145), and one susceptible (91-44) to SSR to complete this study. A comparative analysis using a combination of RNAseq, metabolomics, and chemical genomics in yeast, shows that resistance in 91-145 is associated in part with an earlier induction of jasmonate signaling, increased ability to scavenge ROS, and importantly, a reprogramming of the phenylpropanoid pathway leading to increased antifungal activities. We further discuss and provide evidence for the importance of antifungal compounds during the resistance response against this pathogen and show that this antifungal activity targets ergosterol biosynthesis in the fungus. We propose that the modulation of the identified pathways through RNAi/gene editing or overexpression approaches may be used to introgress SSR resistance in commercial soybean germplasm and possibly other host crops.

RESULTS

Disease development in the resistant (91-145) and susceptible (91-44) soybean lines

To determine soybean processes involved in resistance to SSR, two recombinant inbred lines (RIL) of soybean showing a differential response to *S. sclerotiorum* were chosen for this study. The resistant and susceptible selections were classified based on our previous germplasm selection study (9). Both the resistant 91-145 (R) and the susceptible 91-44 (S) lines were developed utilizing the SSR resistant parental line W04-1002 (P1) and LN89-5717 (PI 5745542), an SSR-susceptible parental line having other desirable pathogen resistance traits (9). Plants were inoculated using the cut petiole inoculation method (16) and infection progression was monitored in R and S soybean lines over seven days. Initial symptoms of SSR began appearing on the main stem 48 hours post-inoculation (hpi) as light brown lesions surrounding the point of inoculation, which spread as the disease progressed. By 96 hpi, extensive tissue colonization occurred along the main stem in the S line, while small restricted lesions with a red coloration were observed at the inoculation site in the R line (Fig. 1). By day 7, it was apparent that the R line had largely restricted fungal growth on the main stem and the red coloration observed at the site of infection had become more prominent, whereas the *S. sclereotiorum* infection had girdled the main stem of the S line (Fig. 1). Global transcriptome analysis was conducted on *S. sclereotiorum* infected soybean stem tissue collected from both R and S lines at 0, 24, 48, and 96 hpi. Metabolomic analysis comparing the R and S lines was also conducted, similarly, stem tissues were collected at 0, 48 and 72 hpi.

Mapping and overview of RNA sequencing data

To determine transcript levels in the R and S soybean lines over the course of infection, RNA sequencing was conducted on twenty-four stem samples, consisting of three independent biological replicates for each of the time points selected. Depending on the time point, 64.9 – 89.7

147 million raw reads were generated, with 95.7 - 96.6% of reads mapping to the host reference
148 genomes of soybean and *S. sclereotiorum* at all timepoints. On average, 96% of the total reads
149 mapped uniquely to the soybean reference genome in the uninfected plants of both lines. In the S
150 line, 91.6, 91.8, and 68.9% of the reads mapped to the soybean genome at 24, 48 and 96 hpi,
151 respectively. In the R line, 92.8, 91.9, and 88.2% of the reads mapped to the soybean genome at
152 24, 48 and 96 hpi, respectively (Table 1). At 96 hpi the reads mapping to the fungal genome in the
153 S line (27%) is significantly higher than those in R line (8%), which is expected considering the
154 extensive colonization of the soybean stem by *S. sclerotiorum* in the S line, particularly at the later
155 stages of the infection process. 4.4 % to 3.2 % of reads at different time point of study did not map
156 to any reference genome and was therefore excluded (data not shown).

157 **Differentially expressed genes (DEGs) of soybean during infection**

158 A comparative analysis of differentially expressed genes (DEGs) was performed during
159 the course of infection in both the R and S lines, as well as between these two lines at the specified
160 time points to investigate the mechanisms underlying resistance to *S. sclerotiorum*. In the R line,
161 we observed the maximum number of DEGs at 48 hours following inoculation (Table S1 and Fig.
162 2A). In contrast, the maximum DEGs in the S line occurred 96 hours post inoculation (Table S1
163 and Fig. 2B). Interestingly, at 96 hpi, the number of DEGs in the S line (14,050) were markedly
164 higher than the R line (2,442), suggesting that the resistant response may be contributing to the
165 reduced differential expression of host genes and the return to homeostasis at the later stages of
166 infection. In total, 16,462 unique DEGs were identified in our lines during the course of infection
167 (Fig. 2C). Among these, 7,319 were differentially regulated in both R and S lines, while 920 were
168 strictly associated with the R line and 8,223 were S line specific (Fig. 2C). These results indicate
169 that *S. sclerotiorum* infection causes a dramatic change in gene expression in soybean (~ 19% of

total annotated genes in *Glycine max* genome), and suggests substantial differences between the resistant and susceptible soybean lines used in this study in response to *S. sclerotiorum* challenge.

Pairwise comparisons of DEGs were performed between R and S soybean lines at the selected time points (Table S2 and Fig. 2D). At 24 and 48 hpi, 1,039 and 803 DEGs were identified between the two lines, respectively. However, the number of DEGs sharply increased to 2,087 at 96 hpi. This is consistent with the distinct patterns of gene expression in the S and R lines at the later stages of infection (Fig. 2 A, B). Among the identified DEGs, 447, 191, and 1541 genes were found to be time-point specific between the R and S lines at 24, 48 and 96 hpi, respectively, while 340 genes were differentially expressed at all time points following pathogen challenge (Table S2 and Fig. 2D). The putative functions of these genes were determined using Phytozome (33), National Center for Biotechnology Information (NCBI), and Soybase (21) databases (Table S2).

Gene ontology enrichment and biological process analyses

We focus the reminder of this manuscript on direct comparisons between resistant and susceptible soybean lines, to single out potential processes associated with resistance to *S. sclerotiorum* in soybean. Soybean gene locus IDs identified through the DEG analysis were used to perform gene ontology (GO) enrichment analysis using the Soybase gene model data mining and analysis tool (34). A false discovery rate (FDR) value of 0.05 was used to identify significantly regulated GO biological processes, and individual GO processes were considered in this analysis if they were significantly enriched in at least one of the time points used (Table S3 and Fig. 3). The under or overrepresentation of DEGs in each GO category was determined based on the relative frequencies of the GO terms associated with the genes (34). Our data show an overrepresentation of genes in GO terms related to signal transduction (i.e. kinase signaling, phosphorylation), plant defense responses (i.e. response to chitin, fungi), phenylpropanoid

pathway (i.e. chalcones, anthocyanins, flavonoids, salicylic acid), ROS scavenging, and the biosynthesis/regulation of phytohormones (i.e. jasmonic acid, salicylic acid, ethylene). DEGs underrepresented throughout the course of infection include gene related to nucleotide binding and zinc ion binding. While the involvement of categories such as ROS, defense responses, and phytohormone regulation are not surprising, our results point to complex mechanisms of gene regulation associated with resistance to *S. sclerotiorum*. The differential regulation of phenylpropanoid pathway genes is intriguing and will be the subject of further characterization below.

Metabolite profiling of susceptible and resistant soybean lines in response to *S. sclerotiorum*.

Transcriptomic analysis was complemented by metabolite profiling of stem samples collected from our resistant and susceptible soybean lines following *S. sclerotiorum* infection. Simple changes in transcript levels might not always correlate with biological activity, but changes in metabolite flux are quantifiable outcomes that can directly explain disease phenotypes. Gas chromatography-mass spectrometry (GC-MS) analysis was performed to broadly evaluate metabolite profiles in control and infected soybean stems at 48 and 72 hpi. Three independent biological replicates were used for each time point. A total of 360 metabolites were detected, but only 164 could be identified based on available databases (Table S4). Each metabolite was characterized by its distinct retention time and mass to charge ratio (m/z). All the 164 identified metabolites found in infected soybean were also detected in non-inoculated stems and therefore are likely of plant origin. Despite this, we note that as disease progresses, contributions from *S. sclerotiorum* cannot be ruled out.

MetaboAnalyst 3.0 (35) was used for the analysis of the 164 identified metabolites. One-way ANOVA using Fisher's least significant difference method (Fisher's LSD) identified 80

metabolites, the accumulation of which was significantly (FDR <0.05) affected by *S. sclerotiorum* inoculation at 48 and 72 hpi in R- line compared to S- line (Table S5). These metabolites included polar compounds, such as nucleotides, amino acids, alcohols, organic acids, and carbohydrates, along with nonpolar compounds including fatty acids, and long-chain alcohols (Table S5). The multivariate analysis of identified metabolites was performed using Partial Least Squares - Discriminant Analysis (PLS-DA). The first (PC1) and second (PC2) principal components explain 52.7% of the variance. The analysis showed distinct metabolomic profiles at each time point during the course of infection, culminating with the largest segregation of metabolites between the R and S lines at 72 hpi (Fig. S1). The fold change of significantly regulated metabolites during this time course are indicated in Supplementary Table 5. Significantly regulated metabolites were assigned to distinct functional categories according to the chemical groups to which they belong (Table S5) and to specific plant pathways in which they may function (Table S6). Our data revealed several differentially regulated metabolic processes between the R and S lines (Fig. 4). However, those involved in phenylalanine metabolism are particularly interesting given the differential expression of phenylpropanoid pathway genes identified in transcriptomic analysis (Fig. 5A) and the important role of this pathway in plant defense. Indeed, the precursor of the phenylpropanoid pathway, phenylalanine, and downstream intermediate metabolites, such as benzoic acid, caffeic acid, and ferulic acid, are highly accumulated in the stem of the R line compared to the S line following *S. sclerotiorum* infection (Fig. 5B). Overall, the observed parallel between transcriptomics and metabolomics data with respect to the differential modulation of the phenylpropanoid pathway indicates its potential key participation in resistance to *S. sclerotiorum*.

Similar to transcriptomic data, the comparative metabolite profiles also implicated phytohormones in this interaction. Namely, the fatty acids linolenic acid (a precursor of jasmonic

239 acid) and cyanoalanine (an indicator of ethylene biosynthesis) (36,37) are both significantly
240 induced at 48 and 72 hpi, in the R line (Fig. S3). Interestingly, the most highly upregulated
241 metabolite in our R line is mucic acid with an ~86-fold higher accumulation (Table S5). Mucic
242 acid, also referred to as galactaric acid, can be produced by the oxidation of d-galacturonic acid,
243 the main component of pectin.

244 Galactose metabolism and the TCA cycle were the pathways most affected by this analysis,
245 and the metabolites assigned to them were primarily carbohydrates and organic acids, respectively.
246 Interestingly, of the metabolites downregulated in R plants in comparison to S plants, 81.8% (9/11)
247 belonged to one of these two groups (Table S5). Although these metabolites relate to multiple
248 pathways, their downregulation in R plants may be a strategy to reduce *S. sclerotiorum* access to
249 preferable carbon sources. Of the top six potentially affected pathways, three of them (Glyoxylate
250 and dicarboxylate metabolism; Alanine, aspartate and glutamate metabolism; the TCA cycle)
251 contain both fumaric and succinic acid. These organic acids were downregulated at 48 and 72 hpi,
252 respectively, and demonstrate the potentially broad impacts that changes in individual metabolites
253 can have on plant biosynthesis and metabolism.

254 **Reprogramming of the phenylpropanoid pathway in resistance to *S. sclerotiorum*.**

255 Many secondary metabolites derived from multiple branches of the phenylpropanoid
256 pathway, including lignin, isoflavonoid-phytoalexins, and other phenolic compounds such as
257 benzoic acid, have been proposed as important components of defense responses (38,39). In this
258 study, we found differential expression of transcripts and metabolites related to the
259 phenylpropanoid pathway between the R and S soybean lines. At the transcript level, we observed
260 a downregulation of genes encoding phenylalanine ammonia-lyase (PAL), lignin biosynthetic
261 enzymes, ferulate 5-hydroxylase (F5H), N-hydroxycinnamoyl/benzoyltransferase (HCT),

Caffeoyl-CoA O-methyltransferase (CCoAOMT), cinnamoyl-CoA reductase (CCR), cinnamyl alcohol dehydrogenase (CAD), chalcone synthase (CHS), flavonol synthase (FLS), and flavonoid 4'-O-methyltransferase (FOMT) in R line compared to S line (Table 2 and Fig. 5A). Coincidentally, genes coding for enzymes involved in anthocyanin and phytoalexin biosynthesis were upregulated in the R line, these include, anthocyanidin synthase (ANS), anthocyanin acyltransferase (AT), dihydroflavonol reductase (DFR), isoflavone 7-O-glucoside-6"-O-malonyltransferase (IFMaT) isoflavone 7-O-methyltransferase (IOMT), and isoflavone reductase (IFR) (Table 2 and Fig. 5A). Transcript levels of select genes within these pathways were validated using RT-qPCR, thus confirming the RNA-Seq results (Fig. 6).

In accordance with the transcriptomics data, we observed a marked accumulation of the metabolites phenylalanine, a phenylpropanoid pathway precursor, and the lignin intermediates ferulic and caffeic acids in the R line compared to the S line (Fig. 5B). Benzoic acid, a salicylic acid precursor and known antimicrobial compound (40) also accumulated at higher levels in the Res line (Fig. 5B). Increased accumulation of ferulic and caffeic acids is likely due to the downregulation of F5H (Glyma.09G186400) and other downstream enzymes within the lignin pathway (Table 2 and Fig. 5A). We reasoned that the contribution of these ferulates to resistance may be due to their antifungal activity, and their ability to inhibit *S. sclerotiorum* growth was tested *in vitro*. A significant reduction of fungal growth was observed when *S. sclerotiorum* was grown on PDA with increasing concentrations of ferulic acid (Fig. S2). While caffeic acid did not significantly affect colony size, it clearly affected *S. sclerotiorum* growth patterns on PDA with the appearance of abnormal concentric ring growth patterns and premature sclerotia formation (Fig. S2).

While lignification is recognized as a disease resistance mechanism in plants, counterintuitively, our data suggest a reprogramming of the phenylpropanoid pathway away from lignin and towards the accumulation of lignin intermediates, anthocyanins, and phytoalexins in the resistance response against *S. sclerotiorum*. We propose that lignin intermediates, such as caffeic and ferulic acid, and possibly other compounds with antifungal activity are an important component of this response.

ROS scavenging and antioxidant activities are associated with resistance to *S. sclereotiorum*

Reactive oxygen species (ROS) and ROS scavengers play active roles in redox status regulation in biotic stress (41,42). *S. sclerotiorum*, via oxalic acid, is known to upregulate host ROS levels to induce PCD and achieve pathogenic success (11,15,16). Our transcriptomics analysis shows a differential regulation of genes related to ROS scavenging, such as peroxidases, glutathione S-transferases (GSTs), ascorbate oxidases, and superoxide dismutase (SODs), when comparing the R and S soybean lines (Table S8 and Fig. 7). Three *GmGSTs* (Glyma.06G193400, Glyma.02G024600, Glyma.02G024800), two *GmSODs* (Glyma.12G081300, Glyma.12G178800) and five ascorbate oxidases or like proteins (Glyma.05G082700, Glyma.11G059200, Glyma.17G012300, Glyma.17G180400, Glyma.20G051900, Glyma.05G057400) were significantly upregulated in the R line compared to the S line as early as 24 hpi, suggesting a role in preventing oxidative damage imposed by *S. sclerotiorum* (Table S8 and Fig. 7). Peroxidases were also differentially regulated at 24 hpi, with five family members (Glyma.01G19250, Glyma.11G049600, Glyma.11G080300, Glyma.14G201700, Glyma.17G177800) significantly upregulated, however, many others were downregulated in the R line compared to S line (Table S8 and Fig. 7).

We mined our metabolomics data for differentially accumulated metabolites that may serve as ROS scavengers or antioxidants. Dehydroascorbic acid (DHA), the oxidized form of ascorbate, an important antioxidant, was specifically accumulated later in the infection time course (72 hpi), but not at the early stages in the R line (Fig. 7). Similarly, the proline derivative, trans-4-hydroxy-L-proline, a known osmoprotectant and antioxidant (43,44) is significantly accumulated in the R line at the later stages of the infection process (Fig. 7). Proline plays a major role as an antioxidant, owing to its ROS scavenging capacity (45,46). Overall, these results and the earlier observation of anthocyanin induction, point to a marked activation of ROS scavenging and antioxidant processes in the resistant response to *S. sclerotiorum*, presumably to counter to oxidative state imposed by this pathogen.

Jasmonic acid signaling contributes to the resistant response to *S. sclerotiorum*.

During plant-pathogen interactions, phytohormones such as salicylic acid (SA), abscisic acid (ABA), ethylene (ET), and Jasmonic acid (JA), have been shown to regulate plant immune responses (47–50). ET and JA have generally been implicated in the activation of defense responses against necrotrophs (51). Our GO enrichment analysis highlighted DEGs between the R and S lines related to JA/ET biosynthesis and responses (Table S9 and Fig. 3). Metabolic profiling also identified phytohormone-related metabolites that were differentially accumulated during the course of infection between our lines, namely, linolenic acid, a precursor of jasmonic acid, and cyanoalanine, an indicator of ethylene biosynthesis (Fig. S3). Accordingly, we conducted a targeted GC-MS analysis to more accurately estimate the dynamic changes in SA, ABA, cinnamic acid (an intermediate of SA and the phenylpropanoid pathway), and JA precursors and derivatives (12-oxophytodienoic acid (OPDA), and (+)-7-iso-jasmonoyl-L-isoleucine (JA-Ile) in a time course experiment comparing the R and S soybean lines. Distinct patterns of phytohormone accumulation

were identified during the course of infection (Fig. 8). The bioactive form of JA, Jasmonoyl-L-isoleucine (JA-Ile) but not JA, was significantly induced in the R line compared to the S line between 6 and 24 hpi, before decreasing at the later stages of our time course (Fig. 8). Interestingly, JA and JA-Ile levels drastically increased in the S line, albeit at a much later stage of infection (48 – 72 hpi). Thus, this late dramatic surge in JA and JA-Ile in the S line may be perceived as a delayed response to fungal colonization, perhaps after the establishment of infection (Fig. 7). In accordance, OPDA, a precursor of JA, accumulated at significantly higher levels in the S line at 48 – 72 hpi (Fig. 8). This pattern also explains the significant induction of JA biosynthetic transcripts at the later stages of infection observed in the S line (Table S9). Expectedly, SA accumulated to higher levels in the S line throughout the time course (Fig. 8). JA and SA responses are known to be antagonistic in many plant-pathogen interactions (52). *In toto*, phytohormone estimation in the S and R lines following *S. sclerotiorum* challenge suggests that resistance to this pathogen in soybean coincides with an early induction of JA signaling. The timing of this induction appears to be critical to the outcome of this interaction.

Antifungal activity and mode of action of stem extract from the resistant soybean line

Our earlier observation that soybean stems from the R line accumulated metabolites with antifungal activity, such as ferulic and caffeic acids, following *S. sclerotiorum* challenge was intriguing. This resistant response was also associated with the development of a prominent red coloration at the site of infection (Fig. 1). Considering the metabolomics data, we reasoned that total stem extract from the resistant line should also exhibit antifungal activity against *S. sclerotiorum*. To test this hypothesis, we prepared an ethanol extract of stem sections harvested from the R line,10 days post inoculation, that we termed the red stem extract. Equal amount of

353 green stem extracts harvested from non-inoculated plants served as control. The final extracts were
354 diluted in DMSO following ethanol evaporation. *S. sclerotiorum* growth was assayed on potato
355 dextrose broth (PDB) amended with the red stem extract, green stem extract, or DMSO control for
356 48 hours. Fungal biomass as determined by mycelial fresh weight was markedly reduced (12-14
357 fold) in PDB cultures containing the red stem extract compared to PDB amended with the green
358 stem extract or DMSO (Fig. S4 B, C). These results confirm that the resistant response associated
359 with our R line clearly involves the accumulation of antifungal compounds that inhibit *S.*
360 *sclerotiorum* growth.

361 We next examined the mechanism by which the red stem extract inhibits fungal growth by
362 performing chemical genomic profiling in yeast. Chemical genomic profiling is built upon
363 barcoded strains of *Saccharomyces cerevisiae* mutants representing approximately 4000 gene
364 deletions. The use of unique barcodes for each mutant makes this approach compatible with high-
365 throughput screening of drugs using next-generation sequencing (53). Chemical genomic profiling
366 revealed that deletion mutants of genes involved in phospholipid and sterol biosynthesis were
367 significantly sensitive to the red stem extract (Fig. 9A). Mutants of *ERG6*, which encodes a protein
368 in the ergosterol biosynthetic pathway, had the greatest sensitivity to the extract, and this was a
369 highly significant response ($p<1e-7$). *ERG2*, which is also involved in ergosterol biosynthesis, was
370 also significantly sensitive ($p<0.01$). Mutants of *ARO7*, which encode a gene involved in amino
371 acid biosynthesis was significantly sensitive. While *ARO7* is not known to be directly involved in
372 lipid/sterol biosynthesis, it has many genetic interactions with lipid related genes (54). *CHO2* and
373 *OPI3* mutants were also significantly sensitive. Cho2p and Opi3p are both involved in
374 phosphatidylcholine biosynthesis. A deletion mutant of *PAH1* was the most significantly resistant
375 mutant. Pah1p is a phosphatase that regulates phospholipid synthesis. Deletion mutants of *PAH1*

have increased phospholipid, fatty acid and ergosterol ester content (55). Further, in two out of three replicates, the chemical genomic profile of the red stem extract had significant correlation ($p<0.05$) with the profile of fenpropimorph (56), an ergosterol biosynthesis inhibitor that targets *ERG2* and *ERG24* in yeast. Taken together, these data suggest that the red stem extract may exert toxicity by either disrupting enzymes involved in lipid/sterol biosynthesis, or alternatively physically binding membrane lipids and causing cell leakage.

Red stem extract inhibits ergosterol biosynthesis in *S. sclerotiorum*

To test if the red stem extract causes rapid cell lysis like the antifungal compounds amphotericin B (binds ergosterol) and poacic acid (binds glucan), we performed a cell leakage assay. The red stem extract did not cause significant cell permeability (Fig. 9B). The antifungal drug fluconazole inhibits ergosterol biosynthesis but doesn't cause rapid cell permeability as it targets the enzyme Erg11p rather than a membrane or cell wall structure. This result supports the hypothesis that compounds within the red stem extract target ergosterol biosynthetic enzymes. We thus tested if treatment of *S. sclerotiorum* with the red stem extract alters ergosterol production. *S. sclerotiorum* was grown in PDB amended with red stem extract, green stem extract, or DMSO, and ergosterol level was calculated by first calculating the total ergosterol-plus-24(28) DHE (dehydroergosterol) content and then subtracting from the total the amount of absorption due to 24(28) DHE only (57). Ergosterol content of *S. sclerotiorum* mycelia grown in red stem extract was significantly reduced compared to control treatments (Fig. 9C). The results confirm that the red stem extract inhibits the growth of *S. sclerotiorum* by targeting ergosterol biosynthesis in the fungus.

DISCUSSION

Resistance to fungal pathogens with a predominately necrotrophic lifestyle, such as *Sclerotinia sclerotiorum*, is not well understood due to the likely complex network of responses to these pathogens or their determinants. Uncovering key components of these defense responses is essential for the deployment of disease resistant crops. Omics approaches offer a unique opportunity to identify global cellular networks in plants in response to these pathogens. *S. sclerotiorum* is a broad host pathogen that infects over 400 species, mostly dicotyledonous plants. Its pathogenic success most assuredly relies on a broadly effective toolkit that allows it to infect multiple hosts, however, host-specific dialogue between a given host and the pathogen may also be of importance. In this study, we specifically examine soybean resistance mechanisms against *S. sclerotiorum* by comparing opposing outcomes in two soybean lines in response to this pathogen using a combination of transcriptomics, metabolomics, and chemical genomics. Several lines of evidence are consistent with the following conclusions: (i) *S. sclerotiorum* challenge induces drastic changes in gene expression and metabolite production in soybean; (ii) Resistance in soybean is associated with an early recognition of the pathogen and a rapid induction of JA signaling; (iii) The redox buffering capacity of the host is essential to counter the oxidative state imposed by *S. sclerotiorum*; (iv) A reprogramming of the phenylpropanoid pathway and upregulation of antifungal metabolites are observed during the resistant response to *S. sclerotiorum*; (v) The antifungal activity associated with resistance targets ergosterol biosynthesis in the pathogen. Overall, comprehensive genetic, biochemical, and transcriptomic analyses allowed us to uncover a novel resistance mechanism connecting the upregulation of antifungal activity to a successful defense response against *S. sclerotiorum* and highlights the importance of early recognition and redox regulation in resistance to this pathogen.

The importance of ROS in plant immunity and other plant processes, including abiotic stress responses, growth and development, is well documented (58). In plant immunity, ROS can function not only as antimicrobials and in plant cell wall reinforcement, but also as signaling molecules activating additional defense responses (59). The implication of host ROS in plant defenses, including the hypersensitive response (HR) and pathogen-associated molecular pattern (PAMP)-triggered immunity following pathogen recognition is well documented (60,61). However, ROS are also produced during compatible interactions, thus facilitating host colonization of certain fungal pathogens (11,14,16,62). *S. sclerotiorum* is known to induce apoptotic-like PCD via oxalic acid, a process that requires ROS upregulation in the host (15). Indeed, we have recently shown that this pathogen hijacks soybean NADPH oxidases to increase ROS levels leading to tissue death and the establishment of disease, and that the silencing of specific host NADPH oxidases confers enhanced resistance to this pathogen (16). This study confirms the importance of ROS in this pathosystem and suggests ROS scavenging and antioxidant activity as viable resistance mechanisms in soybean. Indeed, we noted the significant upregulation of genes related to ROS scavenging such as peroxidases, glutathione S-transferases, ascorbate oxidases, and superoxide dismutase, in association with the successful defense response against *S. sclerotiorum*. Similar trends were reported in other host and non-host plant species in association with *S. sclerotiorum*, with strong upregulation of genes encoding ROS scavenging enzymes and higher antioxidant enzymatic activities coinciding with resistance to this pathogen (63–66). We also noted the accumulation of antioxidant metabolites dehydroascorbic acid (DHA) and trans-4-hydroxy-L-proline. DHA is converted into ascorbic acid (AA), which is known for its redox buffering capacity and ROS detoxification (67,68). The utilization of ascorbic acid as an antioxidant in cells causes its oxidation back to dehydroascorbic acid (69). Thus, the low levels of

444 DHA in our resistant line at the onset of infection can be explained by higher ascorbic acid levels
445 at this stage. Once oxidized, AA is converted to DHA, which accumulated at the later stages of
446 our time course. Similarly, the proline derivative, trans-4-hydroxy-L-proline, was markedly
447 increased in our resistance response, and is a known osmoprotectant and antioxidant (43,44). The
448 accumulation of proline in plants has been implicated in stress tolerance by maintaining osmotic
449 balance, stabilizing membranes, and modulating ROS levels (43). Overall, our accumulating
450 evidence suggests that the antioxidant capacity of soybean plays a critical role in its ability to resist
451 *S. sclerotiorum*, a pathogen that induces ROS and cell death in the host to achieve pathogenic
452 success.

453 An important question is what causes this stark difference in ROS buffering capacity
454 between the R and S soybean lines despite common genetic components? We propose that the
455 early recognition of the pathogen in the R line leads to a timely response that includes the activation
456 of the antioxidant machinery within the host. This is corroborated by our phytohormone analysis
457 that shows a rapid induction of the bioactive form of jasmonic acid (JA), Jasmonoyl-L-isoleucine
458 (JA-Ile) as early as 6 hpi in the resistance response, JA-Ile levels decreased at the later stages of
459 infection, presumably once the infection was under control. In contrast, in the susceptible response,
460 JA and JA-Ile levels remained low early, but drastically increased at the later stages of our time
461 course, which can be conceived as a delayed and unsuccessful response to fend off an already
462 established infection. A large body of work on plant defenses described the implication of specific
463 hormone pathways depending on pathogen lifestyle (47–50,52). Plant defenses involving JA
464 typically inhibit fungal necrotrophs (52), and mutants specifically impaired in JA-Ile accumulation
465 show enhanced susceptibility to such pathogens (70–72). Our results are consistent with the model
466 where upon *S. sclerotiorum* challenge, JA is rapidly biosynthesized from linolenic acid and

subsequently catalyzed to JA-Ile, the active form of JA. Our metabolomics analysis also showed that linolenic acid is hyper accumulated early in the resistance response. JA-Ile is known to act upon the F-box protein COI1 (Coronatine-insensitive protein 1) leading to the targeting of JAZ (Jasmonate-Zim Domain) proteins for degradation, thus liberating JAZ repressed transcription factors involved in defense (72,73). Thus, while JA signaling appears to be activated in both resistant and susceptible responses, the timing of this induction is key to the resistance outcome in *S. sclerotiorum*-soybean interaction. The early induction likely leads the timely activation of defense components culminating in the arrest of fungal growth and colonization. The reciprocal antagonism between JA and SA signaling pathways is often discussed, and SA signaling is expected to have a negative effect on resistance to pathogens with a predominately necrotrophic lifestyle (52). Our data indicates a higher and sustained levels of SA in the susceptible line throughout our time course, thus in line with the notion that these signaling pathways are antagonistic. SA is also associated with elevated ROS levels and cell death induction, to the benefit of necrotrophic pathogens (74). However, the exact role of SA in this interaction will require further investigation knowing that the crosstalk between JA and SA signaling is complex, and synergistic interactions have also been reported (50).

JA signaling have been linked to the alteration of plant secondary metabolites, including alkaloids, terpenoids, flavonoids, phenolic compounds, and phytoalexins (75–79). Secondary metabolites derived from multiple branches of the phenylpropanoid pathway, including lignins, isoflavonoid-phytoalexins, and other phenolic compounds have also been proposed as important components of defense responses (38,39). The integration of our transcriptomic and metabolic data revealed that the phenylpropanoid pathway is differentially regulated in our soybean lines in response to *S. sclerotiorum* challenge. Specifically, our data suggest a reprogramming of the

490 phenylpropanoid pathway with its flux diverted from lignin to lignin intermediates, anthocyanins,
491 and phytoalexins in the resistance response against *S. sclerotiorum*. While these results will require
492 further confirmation by the absolute quantification of phenylpropanoid pathway components, the
493 accumulation of upstream metabolites such as ferulic acid, caffeic acid, and benzoic acid in the
494 resistance line support a reduced flow towards lignins. The observed accumulation of ferulic acid
495 is also consistent with decreased lignification considering its role as a nucleation site for lignin
496 polymerization (80). These results may seem counterintuitive considering that lignin biosynthesis
497 is associated with cell wall fortification as a mechanism of disease resistance (81). However, in
498 support of our results, a negative correlation between soybean stem lignin content and resistance
499 to *S. sclerotiorum* has previously been reported (32). Flux changes within the phenylpropanoid
500 pathway in maize have been discussed in response to the biotrophic fungal pathogen *Ustilago*
501 *maydis* (82,83). Interestingly, *U. maydis*, via the secreted effector Tin2, diverts the flow of the
502 phenylpropanoid pathway away from lignins by increasing anthocyanin biosynthesis to facilitate
503 infection. In the absence of this effector, lignin biosynthesis is enhanced presumably to limit fungal
504 colonization (83). In contrast to our results, resistance to *U. maydis* appears to be associated with
505 the activation of the lignin branch of the phenylpropanoid pathway. However, these observations
506 are in line with the limited lytic repertoire and the biotrophic lifestyle of *U. maydis*. Against
507 necrotrophic fungal pathogens, anthocyanin may act as antioxidants by scavenging ROS and
508 limiting the induction of cell death required by these pathogens. Indeed, the ROS scavenging
509 capacity of anthocyanins has been proposed to provide protection against necrotrophic pathogens
510 such as *Botrytis cinerea* (84) and *Erwinia carotovora* (85). We propose that this mechanism may
511 also confer resistance against *S. sclerotiorum* in soybean.

512 The reported antimicrobial activities of ferulic (86), caffeic (87), and their significant
513 accumulation in the resistance response against *S. sclerotiorum* prompted us to consider antifungal
514 activity as a component of the soybean defense response against this pathogen. Indeed, total red
515 stem extracts from our resistant line following *S. sclerotiorum* challenge clearly inhibited fungal
516 growth *in vitro*. This antifungal response was seemingly absent from healthy soybean plants,
517 activated only in response to *S. sclerotiorum*. Furthermore, we were able to show using chemical
518 genomics in yeast that factors within this antifungal activity target ergosterol biosynthesis in the
519 fungus. Ergosterol, a lipid found in the cellular membranes of fungi, is important to the regulation
520 of membrane fluidity and permeability. It is therefore conceivable that plants have evolved means
521 to target this key component of fungal membranes. For example, saponins, which affect membrane
522 integrity by tergeting 3β-hydroxyl sterols, were shown to be required for resistance against
523 *Gaeumannomyces graminis* var. *tritici* and several *Fusarium spp* (88–90). Plant antimicrobial
524 peptides and coumarin, a product of the phenylpropanoid pathway, were also proposed to target
525 fungal ergosterol (91,92). The specific metabolites responsible for these antifungal activities in our
526 resistant line are currently unknown. While we provided evidence that both ferulic and caffeic
527 acids affected *S. sclerotiorum* growth, their chemical genomic profile did not match that of the red
528 stem extract. Thus, we propose that other unknown compounds target ergosterol biosynthesis and
529 contribute to resistance to this pathogen. The identification of these compounds through high-
530 resolution mass spectrometry may lead to the discovery of novel bioactive metabolites and help
531 devise specific strategies to introgress resistance to fungal pathogens in crop plants.
532
533
534

535 **METHODS**

536 **Plant material and pathogen inoculation**

537 Two recombinants inbred lines of soybean (*Glycine max*), 91-145 and 91-144, were used in this
538 study. Both the resistant 91-145 (R) and the susceptible 91-44 (S) lines were developed utilizing
539 W04-1002 (P1), a SSR resistant parental line, and LN89-5717 (PI 5745542), a SSR-susceptible
540 parental line demonstrating other desirable pathogen resistance traits (9). Soybean seedlings and
541 plants were maintained in the greenhouse or growth chamber at 24 ± 2℃ with 16-h light/8-h dark
542 photoperiod cycle. Plants were supplemented fertilizer (Miracle-Gro) every two weeks.

543 SSR infection was performed using a wild type strain of *S. sclerotiorum* (1980) grown at
544 room temperature on potato dextrose agar (PDA) as described by Godoy et al. 1990. Four-week-
545 old soybean plants were infected with *S. sclerotiorum* by petiole inoculation, using an agar plug
546 of actively growing fungal hyphae. Plant tissue was sampled by cutting horizontally above and
547 below (1.5 cm) the node of the inoculated petiole with a clean straight-edge razor (16). Tissue
548 samples were then immediately frozen in liquid nitrogen prior to RNA extraction and metabolomic
549 analysis. Samples from non-inoculated stem tissues were also collected as a control. The
550 experimental design was completely randomized and consisted of three biological replicates for
551 each of the treatments. Each biological replicate consisted of stem segments (~3 cm, first
552 internode) from 2 different plants.

553

554 **RNA Extraction and library preparation**

555 Total RNA was extracted from soybean stem tissues using a modified Trizol protocol (Invitrogen
556 Corp., Carlsbad, CA, USA). Briefly, collected tissue from each sample was finely ground in liquid
557 nitrogen. For each 100 mg of tissue, 1 ml of chilled Trizol was added. Samples were centrifuged

558 at 12k rpm for 5 min at 4℃. Supernatant was discarded and 200 µl of chilled chloroform was
559 added, and vortexed at high speed for 15 sec. Samples were centrifuged again at 12k rpm for 15
560 min at 4℃. The aqueous phase was mixed with 0.8x isopropanol and left at room temperature for
561 10 minutes, followed by centrifugation at 12k rpm at 4℃. Supernatant was discarded, and the pellet
562 was washed with 75% ethanol. Pellet was air dried for 10 minutes at room temperature and
563 resuspended in 20µl of nuclease free water followed by incubation at 55℃ for 10 minutes. Samples
564 were cleaned using the RNeasy Plant Mini Kit (Qiagen, Hilden, Germany). RNA concentration
565 and purity were determined by Nanodrop (Thermo Fisher Scientific, Wilmington, DE) and sample
566 quality was assessed using an Agilent Bioanalyzer 2100 and an RNA 6000 Nano Kit (Agilent
567 Technologies, Santa Clara, CA). The RNAseq experiment included three biological replicates per
568 treatment.

569 Library preparation was performed at the University of Wisconsin – Madison
570 Biotechnology Centre (Madison, WI, USA). Individually indexed libraries were prepared using
571 the TruSeq RNA Sample Preparation v2 kit according to the manufacturer's instructions (Illumina,
572 San Diego CA, USA). Library concentrations were quantified with the Qubit HS DNA kit (Thermo
573 Fisher Scientific, Wilmington, DE). The size and quality of the libraries were evaluated with an
574 Agilent Bioanalyzer 2100 and an Agilent DNA 1000 kit (Agilent Technologies, Santa Clara, CA)
575 and the libraries were sequenced using Illumina HiSeq2500 (1X100bp) (Illumina, San Diego CA,
576 USA).

577 **Quality check and sequence analysis**

578 Illumina raw read data quality was verified with fast QC. The soybean and *S. sclereotiorum*
579 genome sequences were acquired from Phytozome v12.1
580 (https://phytozome.jgi.doe.gov/pz/portal.html#! bulk?org=Org_Gmax) and the Broad institute

(https://www.broadinstitute.org/fungal-genome-initiative/sclerotinia-sclerotiorum-genome-project), respectively (10,93). Raw sequence reads were mapped to both genomes using the Subjunc aligner from Subread (94). Alignments were compared to the gene annotation GFF files for both organisms (Soybean: Gmax_275_Wm82.a2.v1.gene.gff3 (93), *S. sclereotiorum*: sclerotinia_sclerotiorum_2_transcripts.gtf (10)) and raw counts for each gene were generated using the feature Counts tool from subread. The raw counts data were normalized using voom from the R Limma package, then used to generate differential expression (log_2FC) values (95,96). DEGs were generated from the comparison of inoculated soybeans of both lines at different time points to their respective uninoculated control (FDR<0.05; log_2FC>1 or <-1).

Gene annotation and gene ontology enrichment analysis

Differentially expressed genes were annotated using soybean genome gene annotations (Annotation_Gmax_275_Wm82.a2.v1.gene.gff3) from Phytozome (https://phytozome.jgi.doe.gov/pz/portal.html#!bulk?org=Org_Gmax) while soybean chloroplast (https://www.ncbi.nlm.nih.gov/nuccore/91214122) and mitochondrion (https://www.ncbi.nlm.nih.gov/nuccore/476507670) sequences were used from NCBI. The statistically significant DEGs (p-value<0.01; log_2FC>1 or <-1) of the R v S comparison were used to identify enriched Gene ontology (GO) terms using the Soybase GO term enrichment tool (https://www.soybase.org/goslimgraphic_v2/dashboard.php) (34).

Metabolites estimation and analysis

Four-week-old soybean plants of susceptible and resistant lines were petiole inoculated as described above. Four stems (3 cm) for each treatment per biological replicate were harvested 48 and 72 hours post inoculation and non-inoculated stems were used as a control. Collected stem

samples were immediately frozen in liquid nitrogen and kept at −80°C until used. Gas chromatographic mass spectrometry (GC-MS) analysis was performed by West Coast Metabolomics (Univ. California, Davis). For metabolite estimation, stem tissue from each treatment was finely ground with liquid nitrogen and extracted with 1 ml of chilled 5:2:2 MeOH: $CHCl_3$: H2O. The aqueous phase was transferred into a new tube and a 500 µl aliquot was dried under vacuum and the residue was derivatized in a final volume of 100 µl. Detailed methods of metabolite derivatization, separation, and detection are described in Fiehn et al., 2016 (97). Briefly, samples were injected (0.5 µl, split less injection) into a Pegasus IV GC (Leco Corp., St Joseph, MI) equipped with a 30 m x 0.25 mm i.d. fused-silica capillary column bound with 0.25 µm Rtx-5Sil MS stationary phase (Restek Corporation, Bellefonte, PA). The injector temperature was 50°C ramped to 250°C by 12°C s-1. A helium mobile phase was applied at a flow rate of 1 ml min^{-1}. Column temperature was 50°C for 1 min, ramped to 330°C by 20°C min-1 and held constant for 5 min. The column effluent was introduced into the ion source of a Pegasus IV TOF MS (Leco Corp., St Joseph, MI) with transfer line temperature set to 230°C and ion source set to 250°C. Ions were generated with a -70 eV and 1800 V ionization energy. Masses (80-500 m/z) were acquired at a rate of 17 spectra s-1. ChromaTOF 2.32 software (Leco Corp) was used for automatic peak detection and deconvolution using a 3 s peak width. Peaks with signal/noise below 5:1 were rejected. Metabolites were quantified by peak height for the quantification ion. Metabolites were annotated with the BinBase 2.0 algorithm (98).

Statistical analyses were conducted in MetaboAnalyst 3.0 (35). Multivariate and univariate statistics were performed on generalized log transformed peak heights. Metabolites with FDR <0.05 were considered differentially regulated. Metabolite pathway analysis was done using the MetaboAnalyst 3.0 Pathway Analysis tool (35).

627 **Reverse Transcriptase–quantitative PCR (RT-qPCR)**

628 The internodal region of the infected petiole (including symptomatic and non-symptomatic tissue)
629 was used for RNA isolation. Stems (3 cm) were harvested and immediately frozen in liquid
630 nitrogen. RNA was isolated using the above-mentioned protocol and then treated with RNase-free
631 DNaseI (NEB Inc., Ipswich, MA, USA). The RNA was reverse transcribed using the AMV First-
632 Strand cDNA Synthesis Kit (NEB Inc., Ipswitch, MA) and oligo-dT primer according to the
633 manufacturer's instructions. RT-qPCR was performed using a SensiFAST SYBR No ROX Kit
634 (Bioline USA Inc., Taunton, MA, USA). Each reaction consisted of 5 µL of SensiFAST SYBR
635 No-ROX Mix, 1µL of 1 : 10-fold diluted template cDNAs, and 0.4 µL of 10 µM gene-specific
636 forward and reverse primers in a final volume of 10 µL. Primers were designed using Primer3
637 software (99,100) for the amplification of gene fragments that were approximately 100 – 200 bp
638 in length and with an annealing temperature of 60°C (Table S7). The primer specificity was
639 checked in silico against the NCBI database through the Primer-BLAST tool
640 (http://www.ncbi.nlm.nih.gov). RT-qPCR was performed on a CFX96 real-time PCR system
641 (Bio-Rad, Hercules, CA). The run conditions were: 2 min of initial denaturation at 95°C; 95°C for
642 5 s, 58°C for 10 s and 72°C for 20 s (40 cycles). The relative expression of genes was calculated
643 using the $2^{-\Delta\Delta Ct}$ method (101) with the soybean gene GmCon15S (102) as an endogenous control.
644 Three biological replicates were used for each sample.
645
646 **Targeted GC-MS analysis of CA, SA, JA, JA-Ile, cis-OPDA, and ABA**
647 Four-week-old soybean plants of susceptible and resistant lines were petiole inoculated
648 with actively growing agar plugs of *S. Sclerotiorum*. Four stems (3 cm) for each biological
649 replicate were harvested at 6, 12, 24, 48, and 72 hpi. Uninoculated stems were also collected for

650 the estimation of the basal concentration of the phytohormones. These collected stem samples were
651 immediately frozen with liquid nitrogen and kept at −80°C until used. Stem tissues from each
652 treatment were finely ground with liquid nitrogen and 100 mg of the ground tissue was added to
653 500 µl of phytohormone extraction buffer (1-propanol/water/HCl [2:1:0.002 vol/vol/v]) and 10 µl
654 of 5 µM solution of deuterated internal standards: d-ABA ([2H6](+)-cis,trans-ABA; [Olchem]), d-
655 IAA ([2H5] indole-3- acetic acid, Olchem), d-JA (2,4,4-d3; acetyl-2,2-d2 JA; CDN Isotopes), and
656 d-SA (d6-SA, Sigma) and analyzed using GC-MS (103–105). The simultaneous detection of
657 several hormones was accomplished using the methods described in Muller et al 2011 with
658 modifications (106). The analysis utilized an Ascentis Express C-18 Column (3 cm × 2.1 mm, 2.7
659 µm) connected to an API 3200 LC-electrospray ionization-tandem mass spectrometry (MS/ MS)
660 with multiple reaction mentoring (MRM). The injection volume was 2 µl and had a 600 µl/min
661 mobile phase consisting of Solution A (0.05% acetic acid in water) and Solution B (0.05% acetic
662 acid in acetonitrile) with a gradient consisting of (time – %B): 0.3 – 1%, 2 – 45%, 5 – 100%, 8 –
663 100%, 9 – 1%, 11 – stop. Three biological replicates of each treatment were performed.
664
665 **Plate inhibition assay of *S. sclerotiorum***
666 The plate growth inhibition assay of *S. sclerotiorum* was done on solid PDA culture plates
667 containing 0, 250, 500, or 1000 µg/mL of ferulic or caffeic acid. Three replicates were used for
668 each treatment. Plates were inoculated with an actively growing plug of *S. sclerotiorum* and grown
669 at 25 °C for either 48 hours (ferulic acid) or 7 days (caffeic acid) prior to assessment.
670
671 **Compound extraction from soybean stem**

672 Five hundred mg of infected red stem or unaffected green stem was mixed 1:1 w/v in 100% ethanol
673 at 80°C for 1 h. Samples were resuspended with 100 µl of DMSO and used for *S. sclerotiorum*
674 inhibition assay, chemical genomics, and cell permeability assays.

675

676 **Chemical genomic analysis**

677 Chemical genomic analysis of the red stem extract was performed using the non-essential yeast
678 deletion mutant collection as described previously (53). Briefly, triplicate 200 µL cultures of the
679 pooled deletion collection were exposed to a 1:10 dilution of the red stem extract and allowed to
680 grow for 48 h. Genomic DNA was extracted using the Invitrogen Purelink 96-well genomic
681 extraction kit (Invitrogen, Carlsbad, CA, USA). Mutant specific barcodes were amplified using
682 indexed primers. Samples were sequenced on a HiSeq2500 (1X50bp) (Illumina, San Diego CA,
683 USA) rapid run and reads were processed using BEAN-counter (107) and EdgeR (108).

684

685 **Cell permeability assay**

686 To quantify the membrane damage caused by the red stem extract a FungaLight™ Cell Viability
687 assay (Invitrogen L34952) and Guava Flow Cytometer (Millipore, USA) was used as described
688 previously (109). Amphotericin B (100 µg/mL) and poacic acid (100 µg/mL) were included as
689 positive controls. Fluconazole (1 mg/mL) was also included as a control, given its ability to inhibit
690 ergosterol biosynthesis without causing rapid cell permeability. We exposed 200 µL log phase
691 populations of yeast cells in YPD media to the control drugs, red stem extract (0.01, 0.005, and
692 0.0025%), the control green stem extract at (0.01, 0.005, and 0.0025%), and a 1% DMSO control

693 (n=3) for 4 h at 30°C. The cells were then stained with the FungaLight™ kit and immediately
694 analyzed by flow cytometry.

695

696 **Biomass and ergosterol estimation of *S. sclerotiorum***

697 The biomass of *S. sclerotiorum* was measured by growing the fungus in potato dextrose broth
698 (PDB). Freshly grown PDA cultures were scraped and then washed twice with water at 4000 rpm
699 (4°C) before being resuspended in water. Equal amounts of resuspended *S. sclerotiorum* were
700 inoculated into 250 mL conical flasks containing 30 mL PDB. For each 30 ml of PDB, 300µl of
701 red stem extract, green stem extract, or DMSO were added and incubated over a period of 48 hours.
702 To estimate the wet weight, the mycelia were filtered on a pre-weighed Miracloth (Darmstadt,
703 Germany). Ergosterol level was estimated as described by Yarden et. al 2014 (57) and Arthington-
704 Skaggs et al 1999 (110). Briefly, mycelia of the *S. sclerotiorum* treated with either red stem extract,
705 green stem extract, or DMSO as described above were washed with distilled water. One gram of
706 mycelium for each strain was resuspended in 3 ml of 25% alcoholic potassium hydroxide solution
707 and vortexed vigorously. Mycelia were then incubated at 85°C for 1 h and sterols extracted by
708 adding 4 ml of n-heptane solution (25% sterile distilled water and 75% n-heptane). The heptane
709 layer was transferred to a clean glass tube and spectrophotometric readings taken between 230 and
710 300 nm. Four biological replicates were used for each treatment. Ergosterol content was calculated
711 as a percentage/g of wet weight using the following equations: % ergosterol + % 24(28)DHE =
712 $[(A_{281.5}/290) \times F]$, % 24(28)DHE = $[(A_{230}/518) \times F]$, where F is the factor for dilution in ethanol
713 and 290 and 518 are the E values determined for crystalline ergosterol and 24(28)
714 dehydroergosterol (DHE), respectively.

Acknowledgments

We thank Grace Brunette and Haley Mesick for their technical assistance. We thank Professor Caitilyn Allen and her group for stimulating discussions. Next-generation sequencing was performed by the Biotechnology Center at the University of Wisconsin-Madison.

References

1. Boland GJ, Hall R. Index of plant hosts of sclerotinia sclerotiorum. Can J Plant Pathol. 1994;16(2):93–108.

2. Baker DG, Burkey AKO, Burton A, Carter TE, Orf JH, Bernardo R, et al. Soybean Pathology White Paper. Crop Sci [Internet]. 2010;103(2):/PHP-2010-1122-01-RS. Available from: https://www.crops.org/publications/cm/abstracts/6/1/0%5Cnhttp://www.pubmedcentral.nih.gov/articlerender.fcgi?artid=3272368&tool=pmcentrez&rendertype=abstract%5Cnhttp://www.pubmedcentral.nih.gov/articleadaprender.fcgi?artid=2586459&tool=pmcentrez&rendertype=ab

3. Peltier AJ, Bradley CA, Chilvers MI, Malvick DK, Mueller DS, Wise KA, et al. Biology, Yield loss and Control of Sclerotinia Stem Rot of Soybean. J Integr Pest Manag [Internet]. 2012;3(2):1–7. Available from: https://academic.oup.com/jipm/article-lookup/doi/10.1603/IPM11033

4. Cunha WG, Tinoco MLP, Pancoti HL, Ribeiro RE, Aragão FJL. High resistance to Sclerotinia sclerotiorum in transgenic soybean plants transformed to express an oxalate decarboxylase gene. Plant Pathol. 2010;59(4):654–60.

5. Hill J, Nelson E, Tilman D, Polasky S, Tiffany D. Environmental, economic, and energetic costs and benefits of biodiesel and ethanol biofuels. Proc Natl Acad Sci [Internet]. 2006;103(30):11206–10. Available from: http://www.pnas.org/cgi/doi/10.1073/pnas.0604600103

6. Ribeiro MDMM, Ming CC, Lopes TIB, Grimaldi R, Marsaioli AJ, Gonçalves LAG. Synthesis of structured lipids containing behenic acid from fully hydrogenated Crambe abyssinica oil by enzymatic interesterification. J Food Sci Technol. 2017;54(5):1146–57.

7. Hartman GL, West ED, Herman TK. Crops that feed the World 2. Soybean-worldwide production, use, and constraints caused by pathogens and pests. Food Secur. 2011;3(1):5–17.

748 8. Hoffman DD, Hartman GL, Mueller DS, Leitz RA, Nickell CD, Pedersen WL. Yield and
749 Seed Quality of Soybean Cultivars Infected with Sclerotinia sclerotiorum. Plant Dis
750 [Internet]. 1998;82(7):826–9. Available from:
751 http://apsjournals.apsnet.org/doi/abs/10.1094/PDIS.1998.82.7.826

752 9. McCaghey M, Willbur J, Ranjan A, Grau CR, Chapman S, Diers B, et al. Development
753 and Evaluation of Glycine max Germplasm Lines with Quantitative Resistance to
754 Sclerotinia sclerotiorum. Front Plant Sci [Internet]. 2017;8(August):1–13. Available from:
755 http://journal.frontiersin.org/article/10.3389/fpls.2017.01495/full

756 10. Amselem J, Cuomo CA, van Kan JAL, Viaud M, Benito EP, Couloux A, et al. Genomic
757 analysis of the necrotrophic fungal pathogens sclerotinia sclerotiorum and botrytis cinerea.
758 PLoS Genet. 2011;7(8).

759 11. Kabbage M, Williams B, Dickman MB. Cell Death Control: The Interplay of Apoptosis
760 and Autophagy in the Pathogenicity of Sclerotinia sclerotiorum. PLoS Pathog. 2013;9(4).

761 12. Liang X, Liberti D, Li M, Kim YT, Hutchens A, Wilson R, et al. Oxaloacetate
762 acetylhydrolase gene mutants of Sclerotinia sclerotiorum do not accumulate oxalic acid,
763 but do produce limited lesions on host plants. Mol Plant Pathol. 2015;16(6):559–71.

764 13. Xu L, Xiang M, White D, Chen W. pH dependency of sclerotial development and
765 pathogenicity revealed by using genetically defined oxalate-minus mutants of Sclerotinia
766 sclerotiorum. Environ Microbiol. 2015;17(8):2896–909.

767 14. Williams B, Kabbage M, Kim HJ, Britt R, Dickman MB. Tipping the balance: Sclerotinia
768 sclerotiorum secreted oxalic acid suppresses host defenses by manipulating the host redox
769 environment. PLoS Pathog. 2011;7(6).

770 15. Kim KS, Min J, Dickman MB. Oxalic Acid Is an Elicitor of Plant Programmed Cell Death
771 during Sclerotinia sclerotiorum Disease Development. 2008;21(5):605–12.

772 16. Ranjan A, Jayaraman D, Grau C, Hill JH, Whitham SA, Ané JM, et al. The pathogenic
773 development of Sclerotinia sclerotiorum in soybean requires specific host NADPH
774 oxidases. Mol Plant Pathol. 2018;19(3):700–14.

775 17. Dallal Bashi Z, Hegedus DD, Buchwaldt L, Rimmer SR, Borhan MH. Expression and
776 regulation of Sclerotinia sclerotiorum necrosis and ethylene-inducing peptides (NEPs).
777 Mol Plant Pathol. 2010;11(1):43–53.

778 18. Nováková M, Sa V, Dobrev PI, Valentová O, Burketová L. Plant Physiology and
779 Biochemistry Plant hormones in defense response of Brassica napus to Sclerotinia
780 sclerotiorum e Reassessing the role of salicylic acid in the interaction with a necrotroph.
781 2014;80:308–17.

782 19. Zhu W, Wei W, Fu Y, Cheng J, Xie J, Li G, et al. A Secretory Protein of Necrotrophic
783 Fungus Sclerotinia sclerotiorum That Suppresses Host Resistance. PLoS One. 2013;8(1).

784 20. Pedras MSC, Ahiahonu PWK. Phytotoxin production and phytoalexin elicitation by the
785 phytopathogenic fungus Sclerotinia sclerotiorum. J Chem Ecol. 2004;30(11):2163–79.

786 21. Grant D, Nelson RT, Cannon SB, Shoemaker RC. SoyBase, the USDA-ARS soybean

787 genetics and genomics database. Nucleic Acids Res. 2009;38(SUPPL.1):843–6.

788 22. Kim HS, Diers BW. Inheritance of partial resistance to sclerotinia stem rot in soybean.
789 Crop Sci. 2000;40(1):55–61.

790 23. Arahana VS, Graef GL, Specht JE, Steadman JR, Eskridge KM. Identification of QTLs
791 for Resistance to in Soybean. Crop Sci. 2001;41(1):180.

792 24. Huynh TT, Bastien M, Iquira E, Turcotte P, Belzile F. Identification of QTLs associated
793 with partial resistance to white mold in soybean using field-based inoculation. Crop Sci.
794 2010;50(3):969–79.

795 25. Moellers TC, Singh A, Zhang J, Brungardt J, Kabbage M, Mueller DS, et al. Main and
796 epistatic loci studies in soybean for Sclerotinia sclerotiorum resistance reveal multiple
797 modes of resistance in multi-environments. Sci Rep. 2017;7(1):1–13.

798 26. Wei W, Mesquita ACO, Figueiró A de A, Wu X, Manjunatha S, Wickland DP, et al.
799 Genome-wide association mapping of resistance to a Brazilian isolate of Sclerotinia
800 sclerotiorum in soybean genotypes mostly from Brazil. BMC Genomics. 2017;18(1):1–16.

801 27. Joshi RK, Megha S, Basu U, Rahman MH, Kav NNV. Genome wide identification and
802 functional prediction of long non-coding RNAs responsive to Sclerotinia sclerotiorum
803 infection in Brassica napus. PLoS One. 2016;11(7):1–19.

804 28. Girard IJ, Tong C, Becker MG, Mao X, Huang J, De Kievit T, et al. RNA sequencing of
805 Brassica napus reveals cellular redox control of Sclerotinia infection. J Exp Bot.
806 2017;68(18):5079–91.

807 29. Seifbarghi S, Borhan MH, Wei Y, Coutu C, Robinson SJ, Hegedus DD. Changes in the
808 Sclerotinia sclerotiorum transcriptome during infection of Brassica napus. BMC
809 Genomics. 2017;18(1):1–37.

810 30. Zhuang X, McPhee KE, Coram TE, Peever TL, Chilvers MI. Rapid transcriptome
811 characterization and parsing of sequences in a non-model host-pathogen interaction; pea-
812 Sclerotinia sclerotiorum. BMC Genomics. 2012;13(1):1–19.

813 31. Oliveira MB, de Andrade R V., Grossi-de-Sá MF, Petrofeza S. Analysis of genes that are
814 differentially expressed during the Sclerotinia sclerotiorum-Phaseolus vulgaris interaction.
815 Front Microbiol. 2015;6(OCT):1–14.

816 32. Peltier AJ, Hatfield RD, Grau CR. Soybean stem lignin concentration relates to resistance
817 to Sclerotinia sclerotiorum. Plant Dis. 2009;93:149–54.

818 33. Goodstein DM, Shu S, Howson R, Neupane R, Hayes RD, Fazo J, et al. Phytozome: A
819 comparative platform for green plant genomics. Nucleic Acids Res. 2012;40(D1):1178–
820 86.

821 34. Morales AMAP, van de Mortel M, E TJB, a AB, F RTN, E DN, et al. Transcriptome
822 analyses and virus induced gene silencing identify genes in the Rpp4 -mediated Asian
823 soybean rust resistance pathway. Funct Plant Biol. 2013;40:1029–47.

824 35. Xia J, Sinelnikov I V., Han B, Wishart DS. MetaboAnalyst 3.0-making metabolomics

more meaningful. Nucleic Acids Res. 2015;43(W1):W251–7.

36. Wasternack C, Song S. Jasmonates: Biosynthesis, metabolism, and signaling by proteins activating and repressing transcription. J Exp Bot. 2017;68(6):1303–21.

37. Yip WK, Yang SF. Ethylene biosynthesis in relation to cyanide metabolism. Bot Bull Acad Sin [Internet]. 1998;39(1):1–7. Available from: http://ejournal.sinica.edu.tw/bbas/content/1998/1/bot91-01.pdf

38. Naoumkina MA, Zhao Q, Gallego-Giraldo L, Dai X, Zhao PX, Dixon RA. Genome-wide analysis of phenylpropanoid defence pathways. Mol Plant Pathol. 2010;11(6):829–46.

39. Piasecka A, Jedrzejczak-Rey N, Bednarek P. Secondary metabolites in plant innate immunity: Conserved function of divergent chemicals. New Phytol. 2015;206(3):948–64.

40. Widhalm JR, Dudareva N. A familiar ring to it: Biosynthesis of plant benzoic acids. Mol Plant [Internet]. 2015;8(1):83–97. Available from: http://dx.doi.org/10.1016/j.molp.2014.12.001

41. Sharma P, Jha AB, Dubey RS, Pessarakli M. Reactive Oxygen Species, Oxidative Damage, and Antioxidative Defense Mechanism in Plants under Stressful Conditions. J Bot [Internet]. 2012;2012:1–26. Available from: http://www.hindawi.com/journals/jb/2012/217037/

42. Apel K, Hirt H. REACTIVE OXYGEN SPECIES: Metabolism, Oxidative Stress, and Signal Transduction. Annu Rev Plant Biol [Internet]. 2004;55(1):373–99. Available from: http://www.annualreviews.org/doi/10.1146/annurev.arplant.55.031903.141701

43. Hayat S, Hayat Q, Alyemeni MN, Wani AS, Pichtel J, Ahmad A. Role of proline under changing environments: A review. Plant Signal Behav. 2012;7(11).

44. Kim KH, Jia B, Jeon CO. Identification of trans-4-hydroxy-L-proline as a compatible solute and its biosynthesis and molecular characterization in Halobacillus halophilus. Front Microbiol. 2017;8(OCT):1–11.

45. Smirnoff N, Cumbes QJ. Hydroxyl radical scavening activity of compatible solutes. Phytochimistry. 1989;28(4):1057–60.

46. Matysik J, Alia, Bhalu B, Mohanty P. Molecular mechanisms of quenching of reactive oxygen species by proline under stress in plants. Curr Sci. 2002;82(5):525–32.

47. Bari R, Jones JDG. Role of plant hormones in plant defence responses. Plant Mol Biol. 2009;69(4):473–88.

48. Pieterse CMJ, Van der Does D, Zamioudis C, Leon-Reyes A, Van Wees SCM. Hormonal Modulation of Plant Immunity. Annu Rev Cell Dev Biol [Internet]. 2012;28(1):489–521. Available from: http://www.annualreviews.org/doi/10.1146/annurev-cellbio-092910-154055

49. Robert-Seilaniantz A, Grant M, Jones JDG. Hormone Crosstalk in Plant Disease and Defense: More Than Just JASMONATE-SALICYLATE Antagonism. Annu Rev Phytopathol [Internet]. 2011;49(1):317–43. Available from:

http://www.annualreviews.org/doi/10.1146/annurev-phyto-073009-114447

50. Pieterse CMJ, Leon-Reyes A, Van Der Ent S, Van Wees SCM. Networking by small-molecule hormones in plant immunity. Nat Chem Biol. 2009;5(5):308–16.

51. Veronese P, Chen X, Bluhm B, Salmeron J, Dietrich R, Mengiste T. The BOS loci of Arabidopsis are required for resistance to Botrytis cinerea infection. Plant J. 2004;40(4):558–74.

52. Glazebrook J. Contrasting Mechanisms of Defense Against Biotrophic and Necrotrophic Pathogens. Annu Rev Phytopathol [Internet]. 2005;43(1):205–27. Available from: http://www.annualreviews.org/doi/10.1146/annurev.phyto.43.040204.135923

53. Piotrowski JS, Simpkins SW, Li SC, Deshpande R, Ong I, Myers CL, et al. Chemical Biology. 2015;1263:1–19. Available from: http://link.springer.com/10.1007/978-1-4939-2269-7

54. Costanzo M, VanderSluis B, Koch EN, Baryshnikova A, Pons C, Tan G, et al. A global genetic interaction network maps a wiring diagram of cellular function. Science (80-). 2016;353(6306).

55. Pascual F, Soto-Cardalda A, Carman GM. PAH1-encoded phosphatidate phosphatase plays a role in the growth phase- and inositol-mediated regulation of lipid synthesis in Saccharomyces cerevisiae. J Biol Chem. 2013;288(50):35781–92.

56. Parsons AB, Lopez A, Givoni IE, Williams DE, Gray CA, Porter J, et al. Exploring the Mode-of-Action of Bioactive Compounds by Chemical-Genetic Profiling in Yeast. Cell. 2006;126(3):611–25.

57. Yarden O, Veluchamy S, Dickman MB, Kabbage M. Sclerotinia sclerotiorum catalase SCAT1 affects oxidative stress tolerance, regulates ergosterol levels and controls pathogenic development. Physiol Mol Plant Pathol [Internet]. 2014;85:34–41. Available from: http://dx.doi.org/10.1016/j.pmpp.2013.12.001

58. Tripathy BC hara., Oelmüller R. Reactive oxygen species generation and signaling in plants. Plant Signal Behav. 2012;7(12):1621–33.

59. Waszczak C, Carmody M. Reactive Oxygen Species in Plant Signaling. 2009;(February):1–28. Available from: http://link.springer.com/10.1007/978-3-642-00390-5

60. Zurbriggen MD, Carrillo N, Hajirezaei MR. ROS signaling in the hypersensitive response: When, where and what for? Plant Signal Behav. 2010;5(4):393–6.

61. Keinath NF, Kierszniowska S, Lorek J, Bourdais G, Kessler SA, Shimosato-Asano H, et al. PAMP (Pathogen-associated Molecular Pattern)-induced changes in plasma membrane compartmentalization reveal novel components of plant immunity. J Biol Chem. 2010;285(50):39140–9.

62. Gilbert BM, Wolpert TJ. Characterization of the LOV1-mediated, victorin-induced, cell-death response with virus-induced gene silencing. Mol Plant Microbe Interact [Internet]. 2013;26(8):903–17. Available from: http://www.ncbi.nlm.nih.gov/pubmed/23634836

902 63. Wei L, Jian H, Lu K, Filardo F, Yin N, Liu L, et al. Genome-wide association analysis and
903 differential expression analysis of resistance to Sclerotinia stem rot in Brassica napus.
904 Plant Biotechnol J. 2016;14(6):1368–80.

905 64. Wen L, Tan TL, Shu J Bin, Chen Y, Liu Y, Yang ZF, et al. Using proteomic analysis to
906 find the proteins involved in resistance against Sclerotinia sclerotiorum in adult Brassica
907 napus. Eur J Plant Pathol. 2013;137(3):505–23.

908 65. Garg H, Li H, Sivasithamparam K, Barbetti MJ. Differentially Expressed Proteins and
909 Associated Histological and Disease Progression Changes in Cotyledon Tissue of a
910 Resistant and Susceptible Genotype of Brassica napus Infected with Sclerotinia
911 sclerotiorum. PLoS One. 2013;8(6).

912 66. Mei J, Ding Y, Li Y, Tong C, Du H, Yu Y, et al. Transcriptomic comparison between
913 Brassica oleracea and rice (Oryza sativa) reveals diverse modulations on cell death in
914 response to Sclerotinia sclerotiorum. Sci Rep [Internet]. 2016;6(February):1–11. Available
915 from: http://dx.doi.org/10.1038/srep33706

916 67. Foyer CH. Redox Homeostasis and Antioxidant Signaling: A Metabolic Interface between
917 Stress Perception and Physiological Responses. Plant Cell Online [Internet].
918 2005;17(7):1866–75. Available from:
919 http://www.plantcell.org/cgi/doi/10.1105/tpc.105.033589

920 68. Foyer CH, Noctor G. Oxidant and antioxidant signaling in plants: a re-evaluation of the
921 concept of oxidative stress in a physiological context. Plant, Cell Environ. 2005;28:1056–
922 1071.

923 69. Wilson JX, Wilson JX. The physiological role of dehydroascorbic acid. FEBS Lett.
924 2002;527(1–3):5–9.

925 70. Agarwal A, Kaul V, Faggian R, Rookes JE, Ludwig-müller J, Cahill DM. Analysis of
926 global host gene expression during the primary phase of the Arabidopsis thaliana –
927 Plasmodiophora brassicae interaction. Funct Plant Biol [Internet]. 2011;38(6):462–78.
928 Available from:
929 http://dx.doi.org/10.1071/FP11026%5Cnhttp://www.publish.csiro.au/?act=view_file&file
930 _id=FP11026.pdf

931 71. Gravot A, Deleu C, Wagner G, Lariagon C, Lugan R, Todd C, et al. Arginase induction
932 represses gall development during clubroot infection in arabidopsis. Plant Cell Physiol.
933 2012;53(5):901–11.

934 72. Yan C, Xie D. Jasmonate in plant defence: Sentinel or double agent? Plant Biotechnol J.
935 2015;13(9):1233–40.

936 73. Pauwels L, Goossens A. The JAZ Proteins: A Crucial Interface in the Jasmonate Signaling
937 Cascade. Plant Cell Online [Internet]. 2011;23(9):3089–100. Available from:
938 http://www.plantcell.org/cgi/doi/10.1105/tpc.111.089300

939 74. Herrera-VÃ¡squez A, Salinas P, Holuigue L. Salicylic acid and reactive oxygen species
940 interplay in the transcriptional control of defense genes expression. Front Plant Sci
941 [Internet]. 2015;6(March):1–9. Available from: http://www.frontiersin.org/Plant-

Microbe_Interaction/10.3389/fpls.2015.00171/abstract

75. Gundlach H, Müller MJ, Kutchan TM, Zenk MH. Jasmonic acid is a signal transducer in elicitor-induced plant cell cultures. Proc Natl Acad Sci U S A [Internet]. 1992;89(6):2389–93. Available from: http://www.pubmedcentral.nih.gov/articlerender.fcgi?artid=48663&tool=pmcentrez&rendertype=abstract

76. Mueller MJ, Brodschelm W, Spannagl E, Zenk MH. Signaling in the elicitation process is mediated through the octadecanoid pathway leading to jasmonic acid. Proc Natl Acad Sci U S A. 1993;90(16):7490–4.

77. Mirjalili N, Linden JC. Methyl Jasmonate Induced Production of Taxol in Suspension Cultures of. Artif Cells Blood Substitutes Immobil Biotechnol Cells Blood Substit Immobi. 1996;110–8.

78. Brader G. Jasmonate-Dependent Induction of Indole Glucosinolates in Arabidopsis by Culture Filtrates of the Nonspecific Pathogen Erwinia carotovora. Plant Physiol [Internet]. 2001;126(2):849–60. Available from: http://www.plantphysiol.org/cgi/doi/10.1104/pp.126.2.849

79. Fugate KK, de Oliveira LS, Ferrareze JP, Bolton MD, Deckard EL, Finger FL. Jasmonic acid causes short- and long-term alterations to the transcriptome and the expression of defense genes in sugarbeet roots. Plant Gene [Internet]. 2017;9:50–63. Available from: http://dx.doi.org/10.1016/j.plgene.2016.12.006

80. Grabber JH, Ralph J, Hatfield RD. Model studies of ferulate - Coniferyl alcohol cross-product formation in primary maize walls: Implications for lignification in grasses. J Agric Food Chem. 2002;50(21):6008–16.

81. Vance C. of Disease Resistance ! 1980;(1).

82. Djamei A, Schipper K, Rabe F, Ghosh A, Vincon V, Kahnt J, et al. Metabolic priming by a secreted fungal effector. Nature. 2011;478(7369):395–8.

83. Tanaka S, Brefort T, Neidig N, Djamei A, Kahnt J, Vermerris W, et al. A secreted Ustilago maydis effector promotes virulence by targeting anthocyanin biosynthesis in maize. Elife. 2014;2014(3):1–27.

84. Zhang Y, Butelli E, De Stefano R, Schoonbeek HJ, Magusin A, Pagliarani C, et al. Anthocyanins double the shelf life of tomatoes by delaying overripening and reducing susceptibility to gray mold. Curr Biol [Internet]. 2013;23(12):1094–100. Available from: http://dx.doi.org/10.1016/j.cub.2013.04.072

85. Lorenc-Kukuła K, Jafra S, Oszmiański J, Szopa J. Ectopic expression of anthocyanin 5-O-glucosyltransferase in potato tuber causes increased resistance to bacteria. J Agric Food Chem. 2005;53(2):272–81.

86. Kumar N, Pruthi V. Potential applications of ferulic acid from natural sources. Biotechnol Reports [Internet]. 2014;4(1):86–93. Available from: http://dx.doi.org/10.1016/j.btre.2014.09.002

87. Matejczyk M, Świsłocka R, Golonko A, Lewandowski W, Hawrylik E. Cytotoxic, genotoxic and antimicrobial activity of caffeic and rosmarinic acids and their lithium, sodium and potassium salts as potential anticancer compounds. Adv Med Sci. 2018;63(1):14–21.

88. Papadopoulou K, Melton RE, Leggett M, Daniels MJ, Osbourn AE. Compromised disease resistance in saponin-deficient plants. Proc Natl Acad Sci [Internet]. 1999;96(22):12923–8. Available from: http://www.pnas.org/cgi/doi/10.1073/pnas.96.22.12923

89. Bednarek, Pawel; Osbourn A. Plant-microbe interactions: chemical diversity in plant defense. Science [Internet]. 2009;324(5928):746–8. Available from: http://www.ncbi.nlm.nih.gov/pubmed/19423814

90. Simons V, Morrissey JP, Latijnhouwers M, Csukai M, Cleaver A, Yarrow C, et al. Dual effects of plant steroidal alkaloids on Saccharomyces cerevisiae. Antimicrob Agents Chemother. 2006;50(8):2732–40.

91. Rautenbach M, Troskie AM, Vosloo JA. Antifungal peptides: To be or not to be membrane active. Biochimie [Internet]. 2016;130:132–45. Available from: http://dx.doi.org/10.1016/j.biochi.2016.05.013

92. Thevissen K, François IEJA, Takemoto JY, Ferket KKA, Meert EMK, Cammue BPA. DmAMP1, an antifungal plant defensin from dahlia (Dahlia merckii), interacts with sphingolipids from Saccharomyces cerevisiae. FEMS Microbiol Lett. 2003;226(1):169–73.

93. Schmutz J, Cannon SB, Schlueter J, Ma J, Mitros T, Nelson W, et al. Genome sequence of the palaeopolyploid soybean. Nature [Internet]. 2010;463(7278):178–83. Available from: http://dx.doi.org/10.1038/nature08670

94. Liao Y, Smyth GK, Shi W. The Subread aligner: Fast, accurate and scalable read mapping by seed-and-vote. Nucleic Acids Res. 2013;41(10).

95. Law CW, Chen Y, Shi W, Smyth GK. Voom: Precision weights unlock linear model analysis tools for RNA-seq read counts. Genome Biol. 2014;15(2):1–17.

96. Ritchie ME, Phipson B, Wu D, Hu Y, Law CW, Shi W, et al. Limma powers differential expression analyses for RNA-sequencing and microarray studies. Nucleic Acids Res. 2015;43(7):e47.

97. Fiehn O. Metabolomics by gas chromatography-mass spectrometry: Combined targeted and untargeted profiling. Vol. 2016, Current Protocols in Molecular Biology. 2016. 1-32 p.

98. Skogerson K, Wohlgemuth G, Barupal DK, Fiehn O. The volatile compound BinBase mass spectral database. BMC Bioinformatics. 2011;12:1–15.

99. Untergasser A, Cutcutache I, Koressaar T, Ye J, Faircloth BC, Remm M, et al. Primer3-new capabilities and interfaces. Nucleic Acids Res. 2012;40(15):1–12.

100. Koressaar T, Remm M. Enhancements and modifications of primer design program Primer3. Bioinformatics. 2007;23(10):1289–91.

101. Livak KJ, Schmittgen TD. Analysis of relative gene expression data using real-time quantitative PCR and the 2-ΔΔCT method. Methods. 2001;25(4):402–8.

102. Libault M, Thibivilliers S, Bilgin DD, Radwan O, Benitez M, Clough SJ, et al. Identification of Four Soybean Reference Genes for Gene Expression Normalization. Plant Genome J [Internet]. 2008;1(1):44. Available from: https://www.crops.org/publications/tpg/abstracts/1/1/44

103. Schmelz EA, Engelberth J, Alborn HT, O'Donnell P, Sammons M, Toshima H, et al. Simultaneous analysis of phytohormones, phytotoxins, and volatile organic compounds in plants. Proc Natl Acad Sci [Internet]. 2003;100(18):10552–7. Available from: http://www.pnas.org/cgi/doi/10.1073/pnas.1633615100

104. Schmelz EA, Kaplan F, Huffaker A, Dafoe NJ, Vaughan MM, Ni X, et al. Identity, regulation, and activity of inducible diterpenoid phytoalexins in maize. Proc Natl Acad Sci [Internet]. 2011;108(13):5455–60. Available from: http://www.pnas.org/cgi/doi/10.1073/pnas.1014714108

105. Christensen SA, Nemchenko A, Park Y-S, Borrego E, Huang P-C, Schmelz EA, et al. The Novel Monocot-Specific 9-Lipoxygenase ZmLOX12 Is Required to Mount an Effective Jasmonate-Mediated Defense Against *Fusarium verticillioides* in Maize. Mol Plant-Microbe Interact [Internet]. 2014;27(11):1263–76. Available from: http://apsjournals.apsnet.org/doi/10.1094/MPMI-06-13-0184-R

106. Müller M, Munné-Bosch S. Rapid and sensitive hormonal profiling of complex plant samples by liquid chromatography coupled to electrospray ionization tandem mass spectrometry. Plant Methods. 2011;7(1):1–11.

107. Piotrowski JS, Li SC, Deshpande R, Simpkins SW, Nelson J, Yashiroda Y, et al. Functional annotation of chemical libraries across diverse biological processes. Nat Chem Biol. 2017;13(9):982–93.

108. Robinson MD, McCarthy DJ, Smyth GK. edgeR: A Bioconductor package for differential expression analysis of digital gene expression data. Bioinformatics. 2009;26(1):139–40.

109. Wyche TP, Piotrowski JS, Hou Y, Braun D, Deshpande R, McIlwain S, et al. Forazoline A: Marine-Derived Polyketide with Antifungal in Vivo Efficacy. Angew Chemie - Int Ed. 2014;53(43):11583–6.

110. Arthington-Skaggs BA, Jradi H, Desai T, Morrison CJ. Quantitation of ergosterol content: Novel method for determination of fluconazole susceptibility of Candida albicans. J Clin Microbiol. 1999;37(10):3332–7.

111. Baxter H, Stewart CN. Effects of altered lignin biosynthesis on phenylpropanoid metabolism and plant stress. Biofuels. 2013;4(6):635–50.

112. Ferrer J-L, Austin MB, Stewart C, Noel JP, Noel JP. Structure and function of enzymes involved in the biosynthesis of phenylpropanoids. Plant Physiol Biochem PPB [Internet]. 2008;46(3):356–70. Available from: http://www.ncbi.nlm.nih.gov/pubmed/18272377%5Cnhttp://www.pubmedcentral.nih.gov/articlerender.fcgi?artid=PMC2860624

List of tables

Table 1. Summary of the sequencing metrics of the RNA-seq.

	Time points (hours)	Total reads	Mapping to *Glycine Max*	Mapping to *S. sclerotiorum*
Susceptible line (S)	Control	79,559,096	76,737,931 (96.5%)	0 (0.0%)
	24 hpi	81,259,978	74,457,988 (91.6%)	3,607,921 (4.4%)
	48 hpi	74,344,340	68,265,965 (91.8%)	2,941,195 (4.0%)
	96 hpi	69,266,099	47,765,044 (68.9%)	18,712,374 (27.0%)
Resistant line (R)	Control	89,753,272	85,133,076 (96.6%)	0 (0.0%)
	24 hpi	64,923,300	60,261,793 (92.8%)	2,286,347 (3.5%)
	48 hpi	67,520,185	62,099,244 (91.9%)	2,513,457 (3.8%)
	96 hpi	72,951,207	64,399,890 (88.2%)	5 691,551 (7.8%)

Table 2. A list of differentially expressed genes (DEGs) within the soybean phenylpropanoid pathway.

Gene locus	24 hpi[a]	48 hpi[a]	96 hpi[a]	Description
Glyma.03G181700	-	-	-1.08	Phenylalanine ammonia-lyase
Glyma.03G181600	-	-0.60	-1.20	Phenylalanine ammonia-lyase
Glyma.02G309300	-	-	-1.28	Phenylalanine ammonia-lyase
Glyma.09G186400	-	-	-1.05	Ferulate 5-hydroxylase
Glyma.04G040000	-	-	-2.08	N-hydroxycinnamoyl transferase
Glyma.01G004200	-	-	-1.32	Caffeoyl-CoA O-methyltransferase
Glyma.05G147000	-	-	-1.54	Caffeoyl-CoA O-methyltransferase
Glyma.19G007200	-	-	-1.12	Cinnamoyl-CoA reductase
Glyma.19G006900	-	-	-1.13	Cinnamoyl-CoA reductase
Glyma.09G201200	-	-	-2.11	Cinnamyl alcohol dehydrogenase
Glyma.02G130400	-	-	-1.05	Chalcone synthase
Glyma.09G075200	-	-	-1.13	Chalcone synthase
Glyma.01G091400	-	-	-1.23	Chalcone synthase
Glyma.08G110500	-1.26	-1.48	-2.05	Chalcone synthase
Glyma.08G110700	-1.25	-1.27	-2.06	Chalcone synthase
Glyma.08G109200	-1.3	-1.58	-2.13	Chalcone synthase
Glyma.08G110400	-1.38	-1.64	-2.18	Chalcone synthase
Glyma.08G110900	-1.12	-1.49	-2.18	Chalcone synthase
Glyma.08G110300	-1.13	-1.5	-2.21	Chalcone synthase
Glyma.16G219400	-	-	-2.23	NAD(P)H-dependent 6'-deoxychalcone synthase
Glyma.08G109300	-1.17	-1.53	-2.24	Chalcone synthase
Glyma.08G109400	-1.3	-1.65	-2.42	Chalcone synthase
Glyma.02G048700	-	-	1.49	Chalcone-flavanone isomerase
Glyma.07G150900	-	-	-2.50	Flavonol synthase
Glyma.18G201900	-	-	-3.77	Flavonol synthase
Glyma.18G267800	-	-5.27	-9.45	Flavonoid 4'-O-methyltransferase
Glyma.11G164700	-	-	2.99	Dihydroflavonol reductase
Glyma.12G238200	-0.88	-0.98	-2.07	Dihydroflavonol reductase
Glyma.11G027700	-	-	3.27	Anthocyanidin synthase
Glyma.01G214200	-	-	2.95	Anthocyanidin synthase
Glyma.02G226000	-	-	1.46	Anthocyanidin 3-O-glucosyltransferase
Glyma.18G271600	3.31	-	-	Anthocyanin acyltransferase
Glyma.13G302300	-	-	2.49	Anthocyanin acyltransferase
Glyma.13G302500	-1.10		-	Anthocyanin 5-aromatic acyltransferase
Glyma.14G034100	-5.85	-3.69	-2.93	Anthocyanin 5-aromatic acyltransferase
Glyma.19G030800	-	-	4.58	Malonyl-CoA:isoflavone 7-O-glucoside-6"-O-malonyltransferase
Glyma.11G256500	-	-	4.61	Isoflavone 7-O-methyltransferase

Glyma.09G094400	-	-1.01	-	Isoflavone-7-O-methyltransferase
Glyma.06G286600	-	-	2.69	Isoflavone 7-O-methyltransferase
Glyma.13G173300	-	-	-1.80	Isoflavone 4'-O-methyltransferase
Glyma.13G173600	-	-	-1.83	Isoflavone 4'-O-methyltransferase

[a] Fold changes (Log_2FC) relative to S line.

Figure Legends

Figure 1. Symptom development in susceptible and resistant soybeans. Disease symptoms observed following petiole inoculation with an agar plug containing actively growing mycelia of *S. sclerotiorum* at 24, 48, 72, 96 hours post-inoculation (hpi) and 7 days post inoculation (dpi). (A) Susceptible (S) line. (B) Resistant (R) line. At 7 dpi in the R line, red coloration at point of inoculation (red node) is prominently visible.

Figure 2. Differentially expressed genes (DEGs) identification in R and S line after *S. sclerotiorum* infection. Venn diagram showing (A) DEGs in R line at 24, 48 and 96 hpi compared to control (non-inoculated) sample, (B) DEGs in S line at 24, 48 and 96 hpi compared to control (non-inoculated) sample, (C) In total, 921 and 8223 DEGs were unique to the R and S line, respectively, while 7319 were identified in both the lines, (D) DEGs in R line compared to S line at 24, 48 and 96 hpi.

Figure 3. Significantly enriched Gene ontology (GO) biological processes in R line compared to S line at different time-points following infection with *S. Sclerotiorum*. The y-axis represents significantly enriched GO processes which were enriched (FDR <0.05) at at-least one time point of infection (24, 48 and 96 hpi). The x-axis indicates the total number of genes annotated to each GO process. Orange sections represent downregulated genes while blue sections represent upregulated genes.

Figure 4. Pathway analysis of metabolites differentially detected between the R and S lines at 48 and/or 72 hpi. The y-axis represents the annotated metabolites in each pathway. Blue sections represent the differentially detected metabolites, whereas green sections represent the remaining annotated metabolites in the pathway. Percentages denote the portion of the pathway found to be differentially detected. Only pathways with at least 10% of their annotated metabolites showing significant regulation were included.

Figure 5. DEGs and metabolites involved in the phenylpropanoid pathway in R and S soybean lines following *S. sclerotiorum* infection. (A) Enzymes are indicated in uppercase letters. Gene names indicated in red or green represent significantly upregulated or downregulated genes in the R line compared to the S line, respectively. The metabolite name in red indicates significantly upregulated phenylpropanoid pathway intermediates in the R line compared to the S line. PAL (phenylalanine ammonia-lyase); BA2H (benzoic acid 2-hydroxylase); C4H (cinnamate 4-hydroxylase); COMT (caffeic O-methyltransferase); F5H (ferulic acid 5-hydroxylase); 4CL (4-coumarate: CoA ligase); C3H (p-coumarate 3 hydroxylase); HCT (N-hydroxycinnamoyl transferase); CCoAOMT (Caffeoyl-CoA O-methyltransferase); F5H (flavanone 5-hydroxylase); CCR (Cinnamoyl-CoA reductase); CAD (Cinnamoyl alcohol dehydrogenase); CHS (chalcone synthase); CHI (chalcone isomerase); CHR (chalcone reductase); FOMT (Flavonoid 4'-O-methyltransferase); FLS (Flavonol synthase); F3H (flavanone 3-hydroxylase); DHFR (dihydroflavonol-4- reductase); ANS (anthocyanidin synthase also called LDOX, leucoanthocyanidin dioxygenase); ANS (Anthocyanidin synthase); UFGT (UDP-flavonoid glucosyltransferase); AT (Anthocyanin acyltransferase); IFS (Isoflavone synthase); IFMaT (Isoflavone 7-O-glucoside-6"-O-malonyltransferase); IOMT (Isoflavone methyltransferase); this figure was adapted from Baxter and Stewart, 2013 (111) and Ferrer et al 2008 (111) (B) Estimation of the phenylpropanoid pathway intermediate metabolites (peak height) phenylalanine, benzoic acid, 3, 4 - dihydroxycinnamic acid (caffeic acid) and ferulic acid in R and S line at 48 and 72 hpi using GC – MS. Data are presented as means ± standard deviation (SD) from three independent biologically replicate with each replicate containing four pooled stem samples. * Indicates a significant difference at p-value < 0.05 (T-Test).

Figure 6. Confirmation of expression profiles of select phenylpropanoid pathway genes using qRT-PCR. (A) PAL (Phenylalanine ammonia-lyase, Glyma.02G309300); (B) HCT (N-hydroxycinnamoyl transferase, Glyma.04G040000); (C) CCoAOMT (Caffeoyl-CoA O-methyltransferase, Glyma.05G147000); (D) CCR (Cinnamoyl-CoA reductase, Glyma.19G006900); (E) CHS (Chalcone synthase, Glyma.08G110400); (F) DHFR (Dihydroflavonol reductase, Glyma.12G238200); (G) ANS (Anthocyanidin synthase, Glyma.11G027700); (H) IOMT (Isoflavone 7-O-methyltransferase, Glyma.11G256500) and (I) AT (Anthocyanin acyltransferase, Glyma.18G271600). The fold changes in expression values for

qRT-PCR were calculated by comparing the expression values of genes in inoculated vs. non-infected soybean stem tissues using the $2^{-\Delta\Delta Ct}$ method. GmCons15 was used as endogenous control. The absolute fold changes were converted to Log_2FC. Data are presented as means ± standard deviation (SD) from three independent experiments.

Figure 7. Reactive oxygen species (ROS) scavenging machinery. (A) Heat map of ROS scavenging (Glutathione S-transferase, Peroxidase, L-ascorbate oxidase, and Superoxide dismutase) and antioxidant genes (Proline-rich protein) induced in the R line compared to the S line during *S. sclerotiorum* infection at 24, 48 and 96 hpi. (B) Differential accumulation of ROS related metabolites trans-4-hydroxy-L-proline and dehydroascorbic acid during *S. sclerotiorum* infection at 48 and 72 hpi. Data are presented as means ± standard deviation (SD) from three independent experiment. * Indicates a significantly difference at p-value < 0.05 (t-test).

Figure 8. Estimation of phytohormones and a phenylpropanoid pathway precursor (Cinnamic acid, CA) in R and S lines following *S. sclerotiorum* infection. (A) Cinnamic Acid (CA), (B) Salicylic Acid (SA), (C) Abscisic Acid (ABA), (D) Jasmonic Acid (JA), (E) JA precursor 12-oxophytodienoic acid (OPDA) and (F) bioactive JA derivative (+)-7-iso-jasmonoyl-L-isoleucine (JA-Ile). The bars represent the standard deviation (n = 3). * Indicates a significant difference between the R and S lines at p-value < 0.05 (One-way ANOVA).

Figure 9. Chemical genomic profiling of the red stem extract in yeast mutants and ergosterol biosynthesis. (A) Plot showing growth differences between yeast deletion mutants exposed to the red stem extract. Dots represent mutants which were significantly sensitive (blue) or resistant (yellow) to the fungicidal activity of the extract. Underlined mutants are implicated in phospholipid and sterol biosynthesis (B) cell leakage assay to test the permeability of *S. sclerotiorum* treated with DMSO, fluconazole (FCZ), amphotericin B (AMB), poacic acid, and different concentrations of green (Cont) and red (Red) stem extract, (C) ergosterol estimation from *S. sclerotiorum* treated with DMSO, green stem extract and red stem extract. Vertical bars show standard deviation of means of three replicates. * Indicates a significant difference at p-value < 0.05 (t-test).

Figure 10. Cellular model summarizing *S. sclerotiorum* resistance mechanisms in soybean. Black line = Induction/suppression of a process, Red line = Secretion/release, Blue line = Bioconversion, Dashed orange line = Translocation of a metabolite, purple asterisk (*) = Downregulation in resistant response, Green asterisk (*) = Upregulation in resistant response, JA = Jasmonic Acid, JA-Ile = Jasmonic Acid-Isoleucine.

Supplementary Figure Legends

Supplementary Figure 1. Partial least squares-discriminate analysis (PLS-DA) score plots of metabolic profiles in soybean R and S line. The first (PC1) and second (PC2) principal components explain 52.7% of the variance. Control samples are R0 and S0. *S. sclerotiorum* infected samples at 24, 48 and 96 hpi for the R lines are represented as R24, R48, and R96, respectively. *S. sclerotiorum* infected samples at 24, 48 and 96 hpi for the S line are represented as S24, S48, and S96, respectively. Numbers 1, 2, and 3 represents three independent biological replicates.

Supplementary Figure 2. Effect of Ferulic and Caffeic acids on *S. sclerotiorum* growth. Ferulic acid (A) inhibits the growth of *S. sclerotiorum*. Representative photographs were taken 48 hours post inoculation. Caffeic acid (B) effects normal development of *S. sclerotiorum*. Representative photographs were taken 5 days post inoculation. DMSO (Dimethyl sulfoxide) is the solvent control.

Supplementary Figure 3. (A) Increased accumulation of the jasmonic acid precursor linolenic acid in the R line compared to the S line, (B) Increased accumulation of cyanoalanine (an indicator of ethylene biosynthesis) in the R line compared to the S line. The bars represent the standard deviation (n = 3). * Indicates a significantly difference at p-value < 0.05 (t-test).

Supplementary Figure 4. (A) Red and green stem extract of a R line plant infected with *S. sclerotiorum* and a S line plant mock inoculated. Extraction was performed 10 dpi, (B) Fungal biomass after growth in PDB cultures containing the red stem extract, DMSO, or green stem

extract, (C) weight of fungal biomass in PDB cultures containing the red stem extract, green stem extract, or DMSO.

List of supplementary tables

Supplementary Table 1. Differentially expressed genes (DEGs) in R and S lines following *S. sclerotiorum* infection at 24, 48, and 96 hpi compared to control. (A-F) Comparisons between each time-point for both lines and their respective controls.

Supplementary Table 2. Differentially expressed genes in the R line compared to the S line following *S. sclerotiorum* infection at 24, 48, and 96 hpi. (A-C) Time-point comparisons between R and S.

Supplementary Table 3. GO enrichment of significant biological processes generated from differentially regulated genes in the R line compared to the S line. (A-C) GO processes identified through the comparison of the R and S lines at 24, 48, and 96 hpi, (D) Summary of significantly regulated genes belonging to each process at each time-point. Processes were included if they had a FDR<0.05 in at-least one timepoint.

Supplementary Table 4. Estimated gas chromatography – mass spectrometry (GC-MS) peak intensity list of all the metabolites.

Supplementary Table 5. Significantly regulated metabolites in the R line compared to the S line following *S. sclerotiorum* infection at 24, 48, and 96 hpi. Blue = upregulated. Red = downregulated.

Supplementary Table 6. Metabolic pathways assigned to significantly regulated metabolites from comparison of R and S lines at 48 and 72 hpi. (A) Percentage of all annotated metabolites within each pathway which were found to be significantly regulated in this study. Upregulated = Green. Downregulated = Red, (B) Fold changes of the individual metabolites assigned to each pathway.

Values >1 demonstrate upregulation. Value <1 demonstrate downregulation. Values =1 demonstrate no change.

Supplementary Table 7. Primer list for qRT-PCR of phenylpropanoid genes

Supplementary Table 8. Differentially expressed genes encoding putative reactive oxygen species (ROS) scavenging and antioxidant genes in the R line compared to the S line following *S. sclerotiorum* infection at 24, 48, and 96 hpi.

Supplementary Table 9. Differentially expressed genes encoding putative jasmonic acid (JA) and ethylene (ET) biosynthetic and response genes in the R line compared to the S line following *S. sclerotiorum* infection at 24, 48, and 96 hpi.

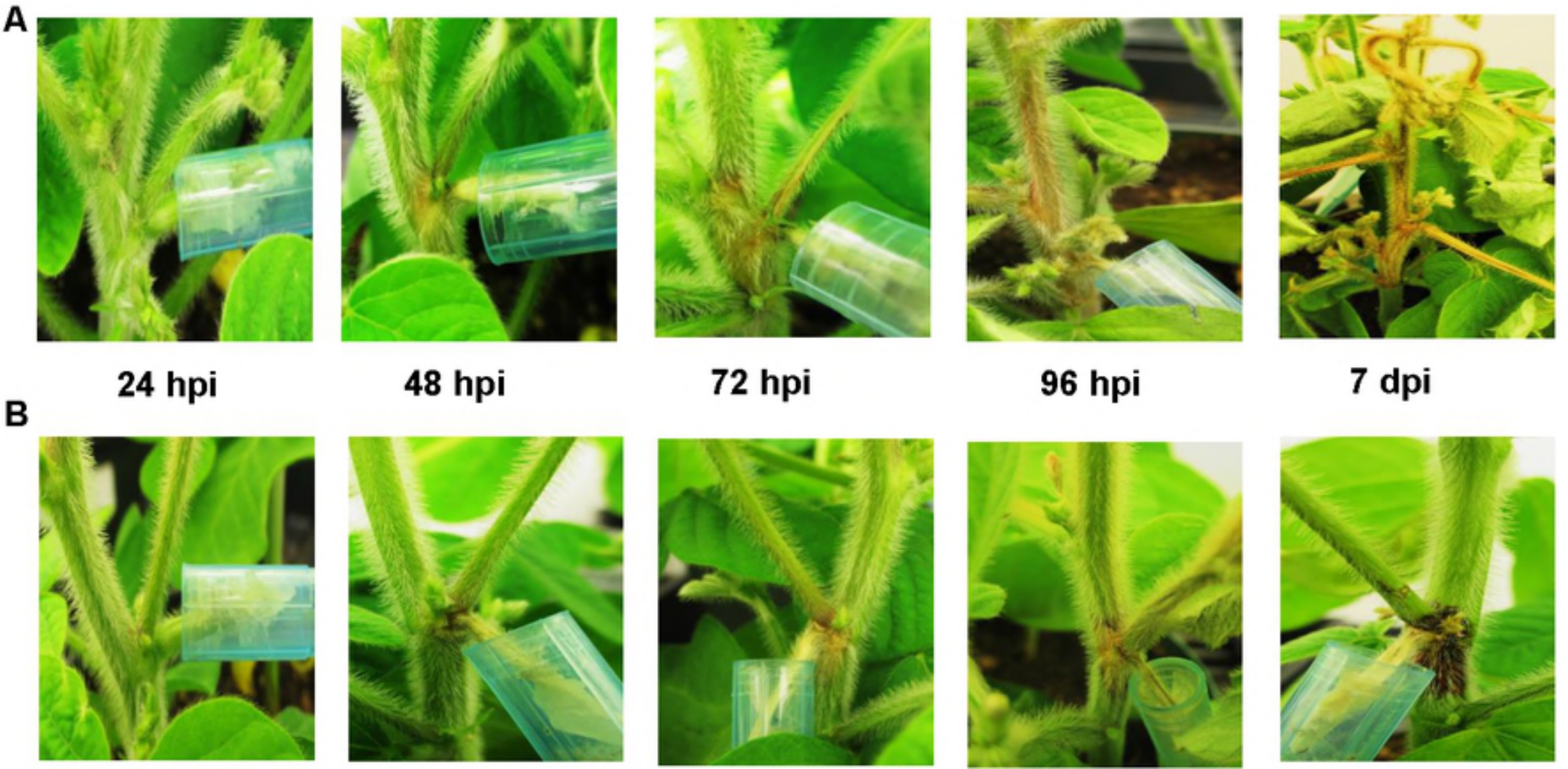
A
24 hpi
48 hpi
72 hpi
96 hpi
7 dpi
B

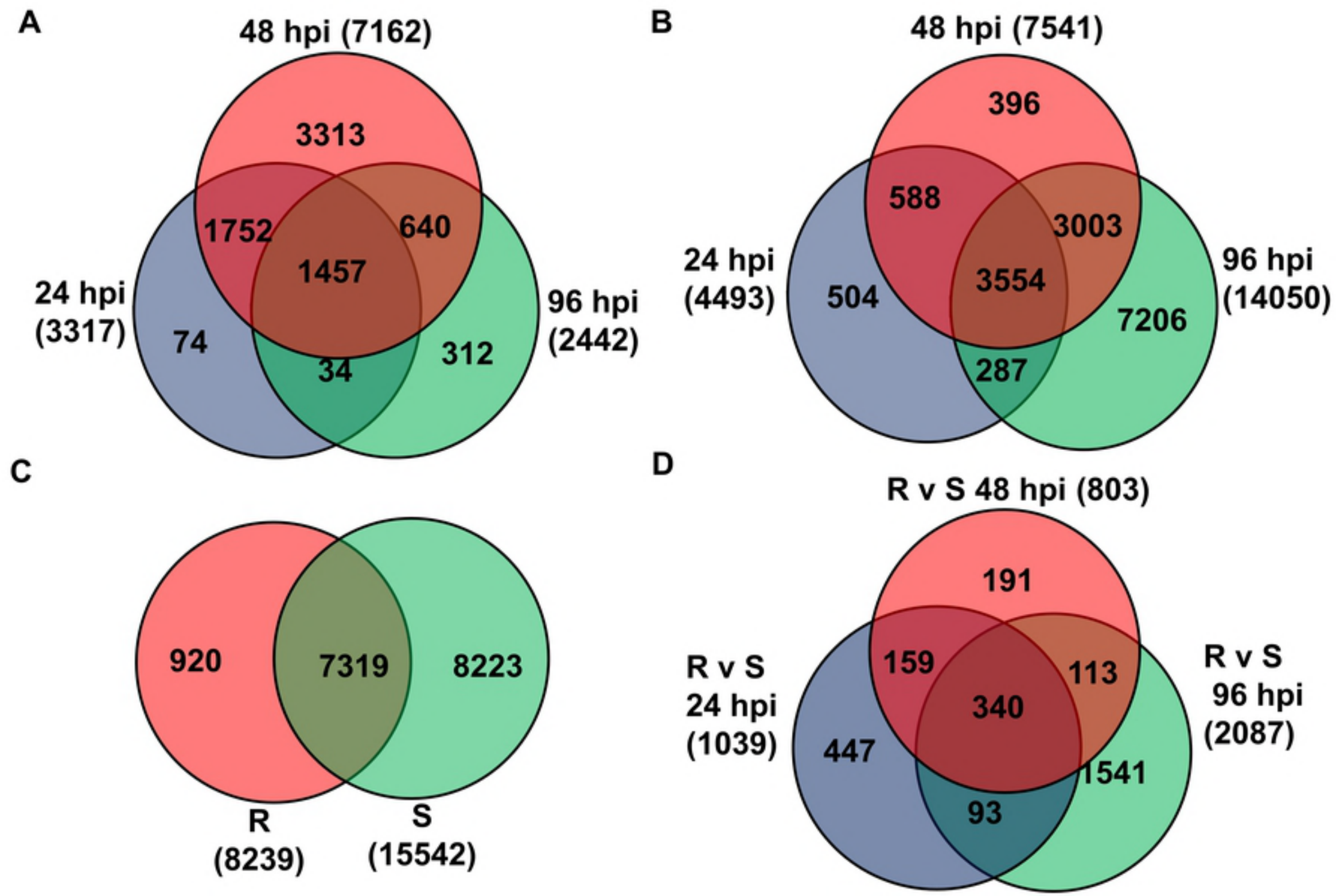
A
48 hpi (7162)
3313
1752
640
1457
24 hpi
(3317)
74
34
312
96 hpi
(2442)
B
48 hpi (7541)
396
588
3003
24 hpi
(4493)
504
3554
7206
96 hpi
(14050)
287
C
920
7319
8223
R
(8239)
S
(15542)
D
R v S 48 hpi (803)
191
159
113
R v S
24 hpi
(1039)
340
447
1541
R v S
96 hpi
(2087)
93

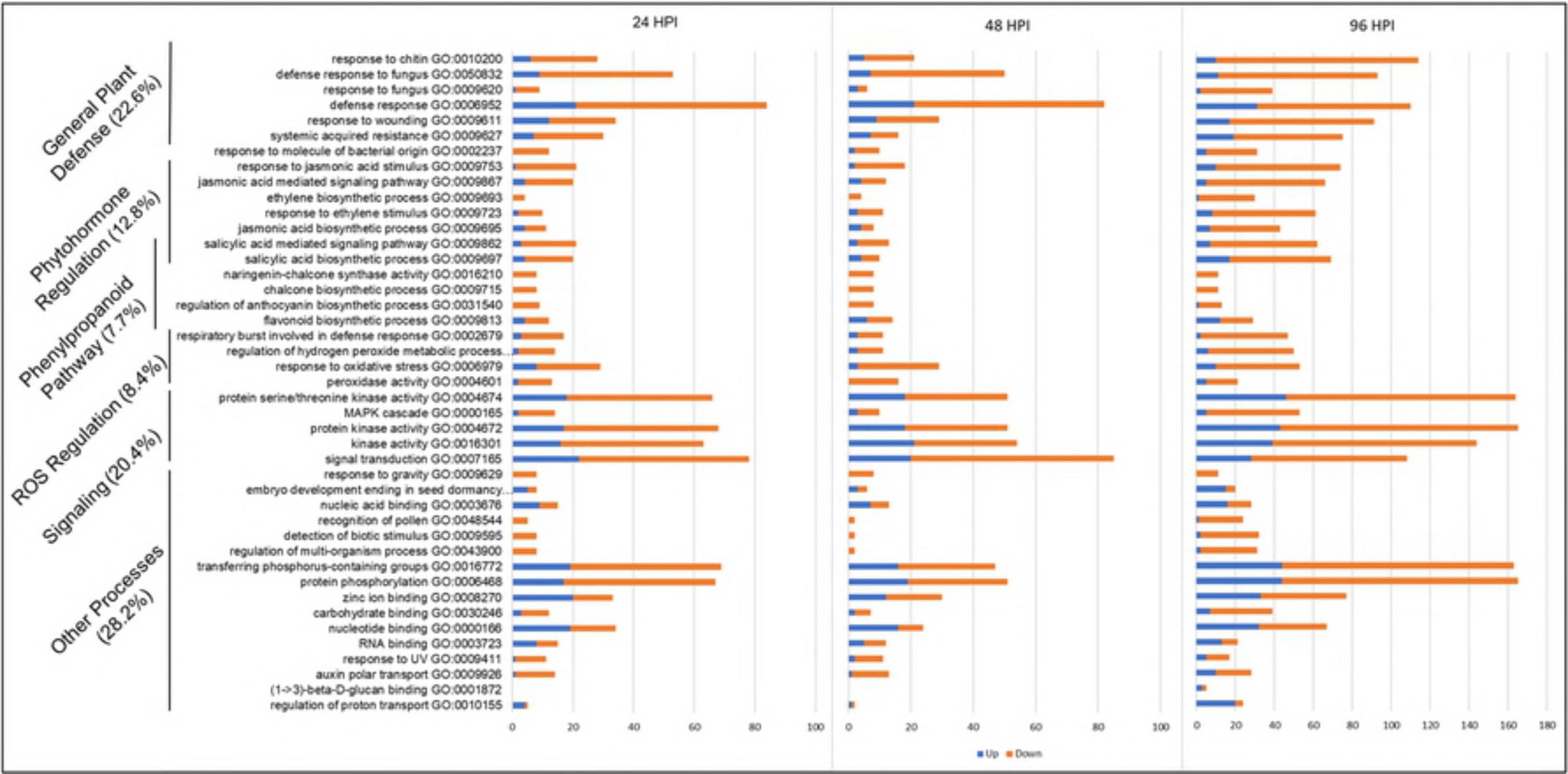
24 HPI
48 HPI
96 HPI
General Plant Defense (22.6%)
Phytohormone Regulation (12.8%)
Phenylpropanoid Pathway (7.7%)
ROS Regulation (8.4%)
Signaling (20.4%)
Other Processes (28.2%)
response to chitin GO:0010200
defense response to fungus GO:0050832
response to fungus GO:0009620
defense response GO:0006952
response to wounding GO:0009611
systemic acquired resistance GO:0009627
response to molecule of bacterial origin GO:0002237
response to jasmonic acid stimulus GO:0009753
jasmonic acid mediated signaling pathway GO:0009867
ethylene biosynthetic process GO:0009693
response to ethylene stimulus GO:0009723
jasmonic acid biosynthetic process GO:0009695
salicylic acid mediated signaling pathway GO:0009862
salicylic acid biosynthetic process GO:0009697
naringenin-chalcone synthase activity GO:0016210
chalcone biosynthetic process GO:0009715
regulation of anthocyanin biosynthetic process GO:0031540
flavonoid biosynthetic process GO:0009813
respiratory burst involved in defense response GO:0002679
regulation of hydrogen peroxide metabolic process...
response to oxidative stress GO:0006979
peroxidase activity GO:0004601
protein serine/threonine kinase activity GO:0004674
MAPK cascade GO:0000165
protein kinase activity GO:0004672
kinase activity GO:0016301
signal transduction GO:0007165
response to gravity GO:0009629
embryo development ending in seed dormancy...
nucleic acid binding GO:0003676
recognition of pollen GO:0048544
detection of biotic stimulus GO:0009595
regulation of multi-organism process GO:0043900
transferring phosphorus-containing groups GO:0016772
protein phosphorylation GO:0006468
zinc ion binding GO:0008270
carbohydrate binding GO:0030246
nucleotide binding GO:0000166
RNA binding GO:0003723
response to UV GO:0009411
auxin polar transport GO:0009926
(1->3)-beta-D-glucan binding GO:0001872
regulation of proton transport GO:0010155
0 20 40 60 80 100
0 20 40 60 80 100
0 20 40 60 80 100 120 140 160 180
Up
Down

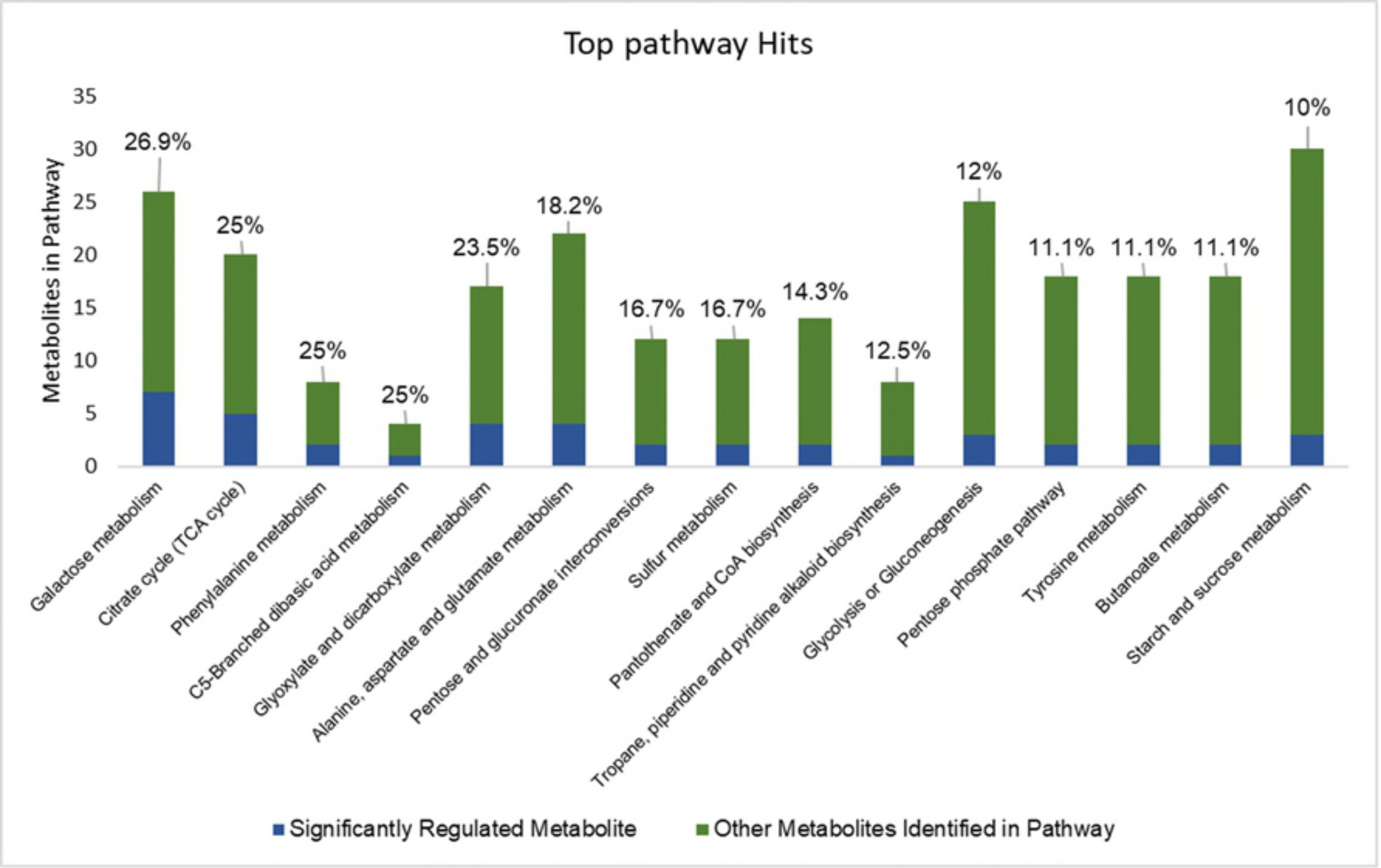
Top pathway Hits
Metabolites in Pathway
35
30
25
20
15
10
5
0
26.9%
25%
25%
25%
23.5%
18.2%
16.7%
16.7%
14.3%
12.5%
12%
11.1%
11.1%
11.1%
10%
Galactose metabolism
Citrate cycle (TCA cycle)
Phenylalanine metabolism
C5-Branched dibasic acid metabolism
Glyoxylate and dicarboxylate metabolism
Alanine, aspartate and glutamate metabolism
Pentose and glucuronate interconversions
Sulfur metabolism
Pantothenate and CoA biosynthesis
Tropane, piperidine and pyridine alkaloid biosynthesis
Glycolysis or Gluconeogenesis
Pentose phosphate pathway
Tyrosine metabolism
Butanoate metabolism
Starch and sucrose metabolism
Significantly Regulated Metabolite
Other Metabolites Identified in Pathway

A

L-Phenylalanine PAL Cinnamic Acid Benzoic Acid BA2H Salicylic Acid

C4H

p- Coumaric Acid

4CL

p- Coumaroyl CoA

CHI/CHR/CHS

IFS

Isoflavones (Phytoalexins)

IFMaT IOMT

Isoflavanones (Phytoalexins)

3 Malonyl CoA CHS

Narigenin Chalcone

CHI

Narigenin

FOMT F3H FLS

Flavonoids Flavonols

DFR

LDOX ANS

UFGT

AT

Anthocyanins

CCR

HCT

p- Coumaroyl Shikimic acid Quinic acid

C3H

Caffeoyl Shikimic acid Quinic acid

p- Coumaraldehyde

CAD

p- Coumaryl alcohol

H Lignin

Caffeic Acid COMT Ferulic Acid F5H 5- Hydroxy Ferulic Acid COMT Sinapic Acid

4CL 4CL 4CL 4CL

HCT

Caffeoyl CoA CCoAOMT Feruloyl CoA F5H 5- Hydroxy Conifery-CoA COMT Sinapoyl-CoA

CCR CCR CCR

Coniferaldehyde 5- Hydroxy Coniferaldehyde Sinapaldehyde

CAD CAD CAD

Coniferyl Alcohol F5H 5- Hydroxy Conifery alcohol COMT Sinapyl alcohol

G Lignin S Lignin

B

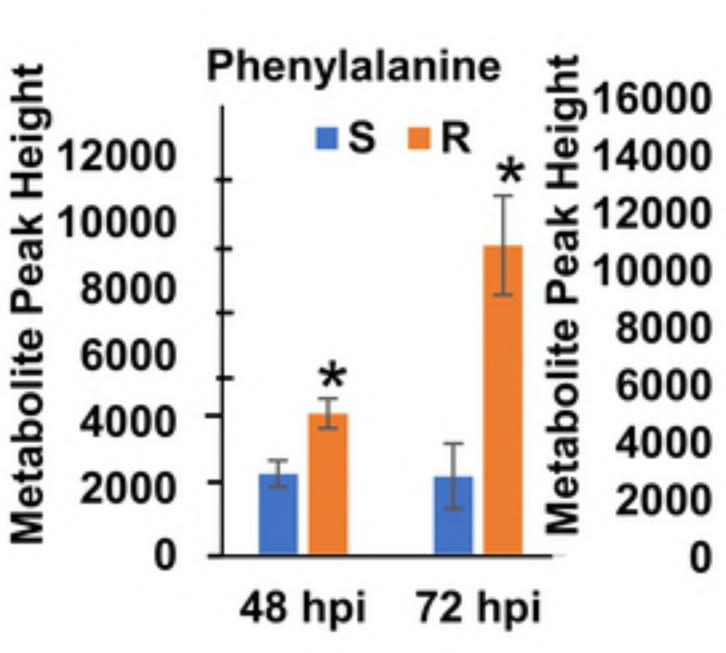

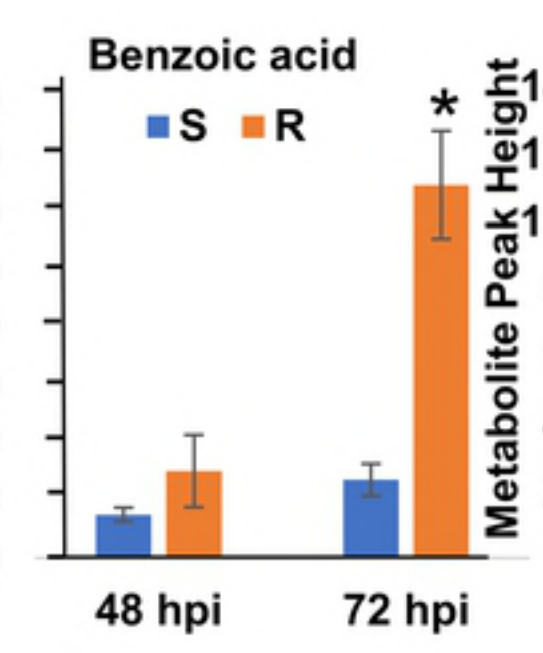

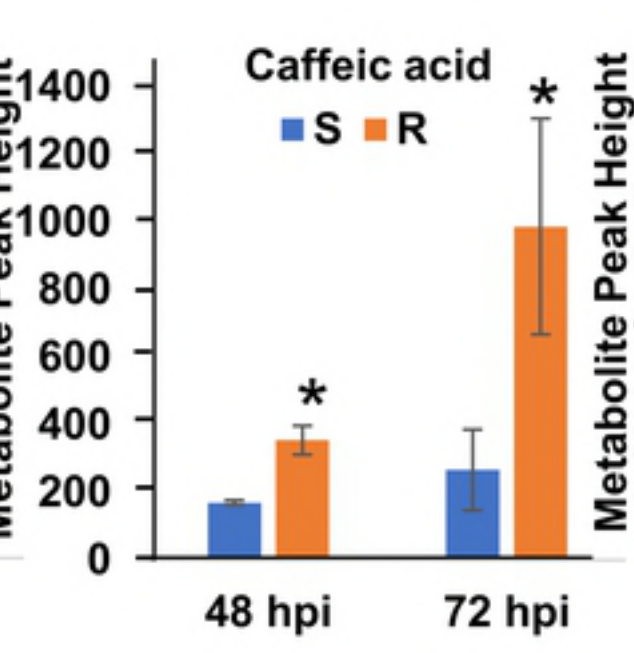

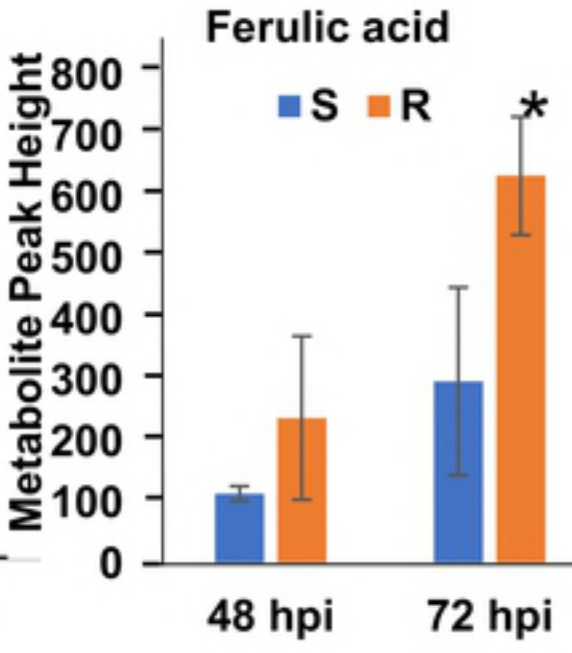

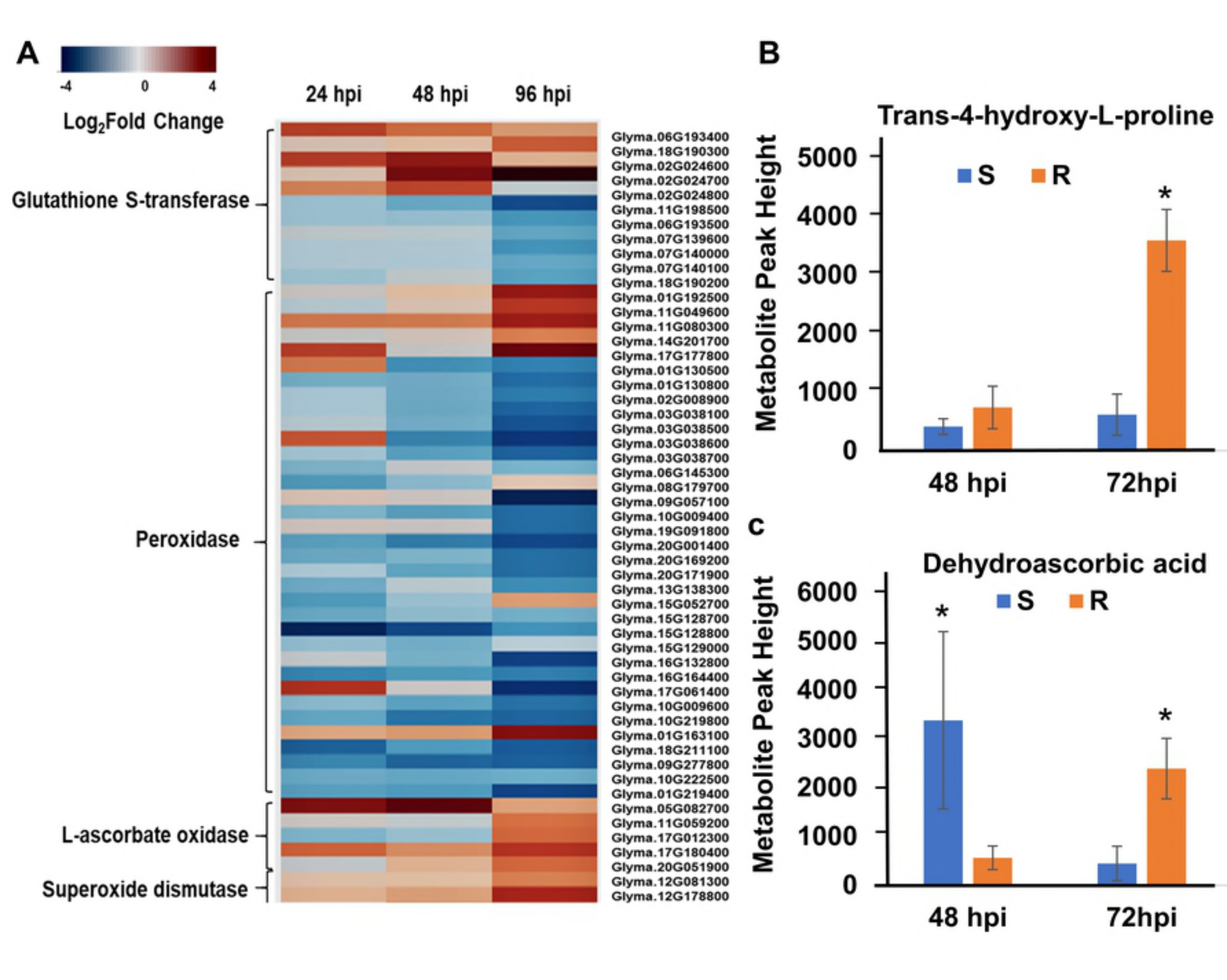
A
-4
0
4
Log2Fold Change
24 hpi
48 hpi
96 hpi
Glutathione S-transferase
Peroxidase
L-ascorbate oxidase
Superoxide dismutase
Glyma.06G193400
Glyma.18G190300
Glyma.02G024600
Glyma.02G024700
Glyma.02G024800
Glyma.11G198500
Glyma.06G193500
Glyma.07G139600
Glyma.07G140000
Glyma.07G140100
Glyma.18G190200
Glyma.01G192500
Glyma.11G049600
Glyma.11G080300
Glyma.14G201700
Glyma.17G177800
Glyma.01G130500
Glyma.01G130800
Glyma.02G008900
Glyma.03G038100
Glyma.03G038500
Glyma.03G038600
Glyma.03G038700
Glyma.06G145300
Glyma.08G179700
Glyma.09G057100
Glyma.10G009400
Glyma.19G091800
Glyma.20G001400
Glyma.20G169200
Glyma.20G171900
Glyma.13G138300
Glyma.15G052700
Glyma.15G128700
Glyma.15G128800
Glyma.15G129000
Glyma.16G132800
Glyma.16G164400
Glyma.17G061400
Glyma.10G009600
Glyma.10G219800
Glyma.01G163100
Glyma.18G211100
Glyma.09G277800
Glyma.10G222500
Glyma.01G219400
Glyma.05G082700
Glyma.11G059200
Glyma.17G012300
Glyma.17G180400
Glyma.20G051900
Glyma.12G081300
Glyma.12G178800
B
Trans-4-hydroxy-L-proline
Metabolite Peak Height
5000
4000
3000
2000
1000
0
S
R
*
48 hpi
72hpi
c
Dehydroascorbic acid
Metabolite Peak Height
6000
5000
4000
3000
2000
1000
0
S
R
*
*
48 hpi
72hpi

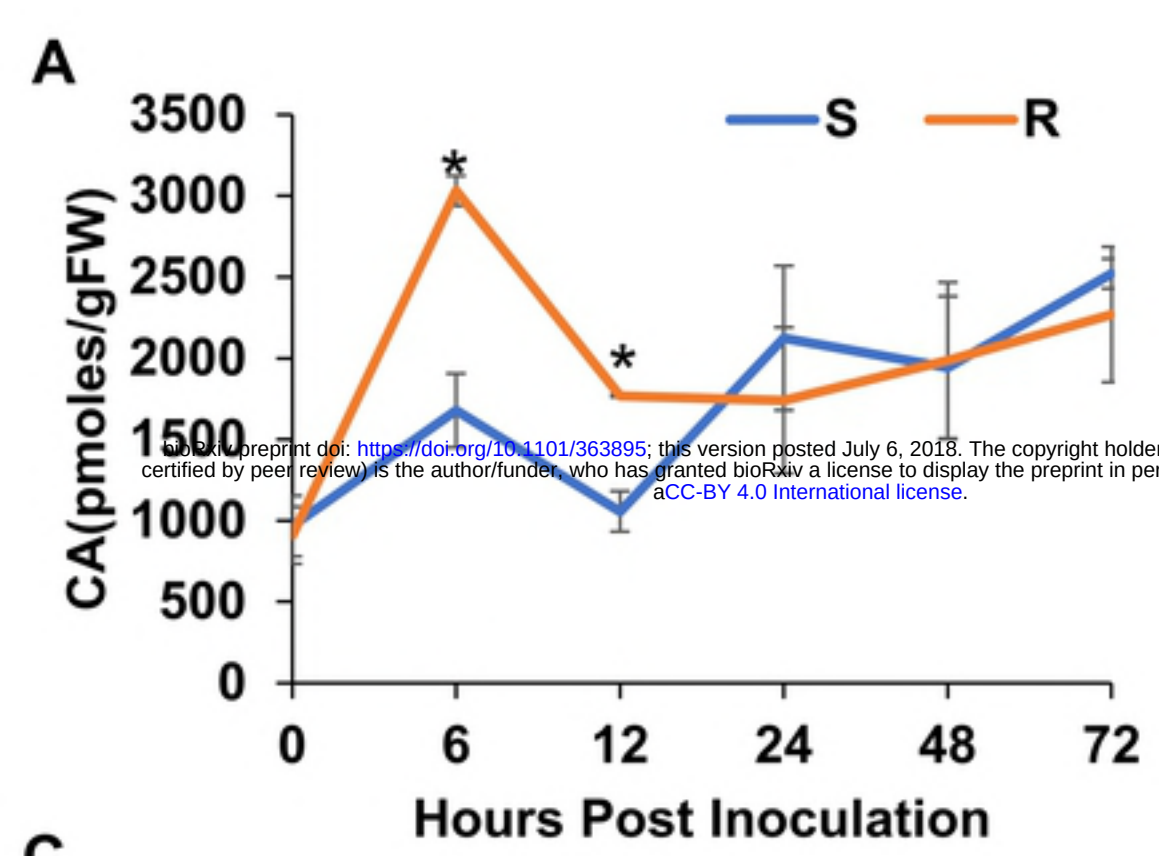

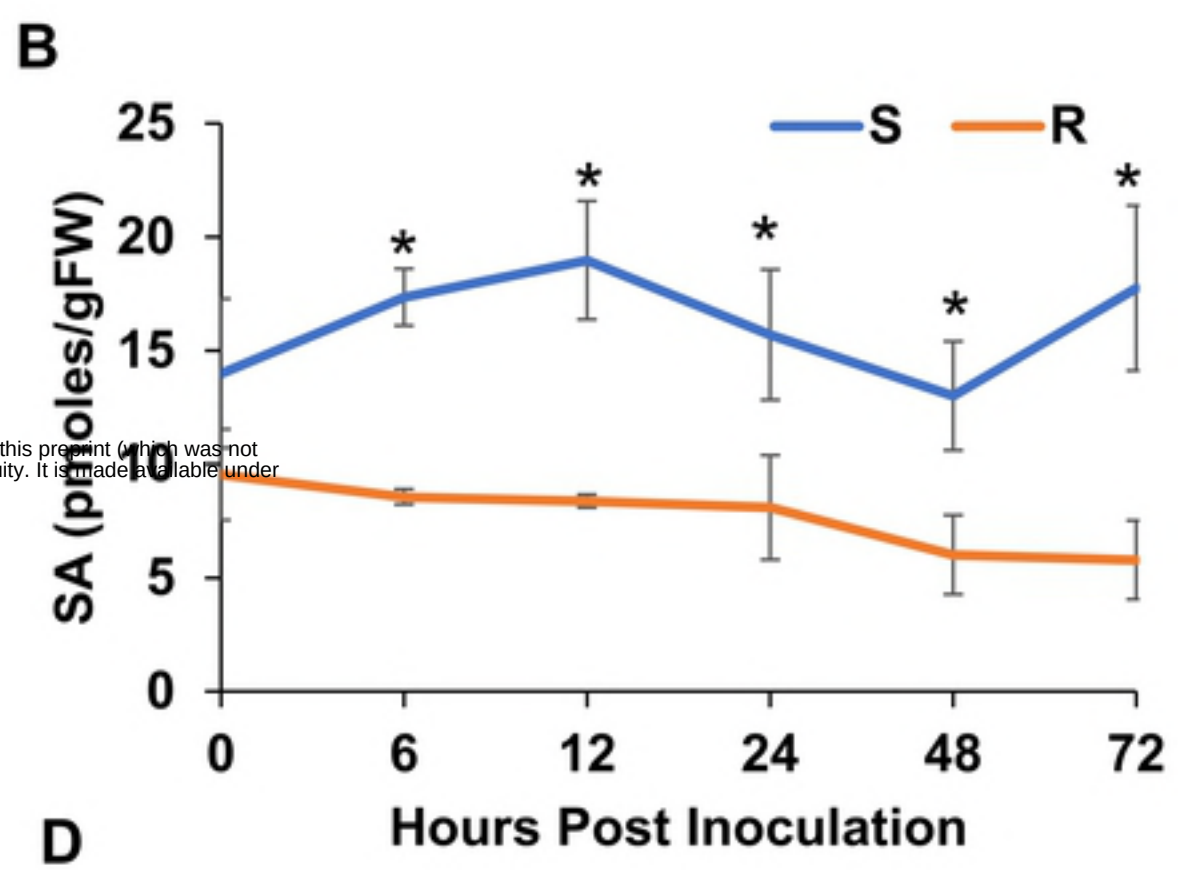

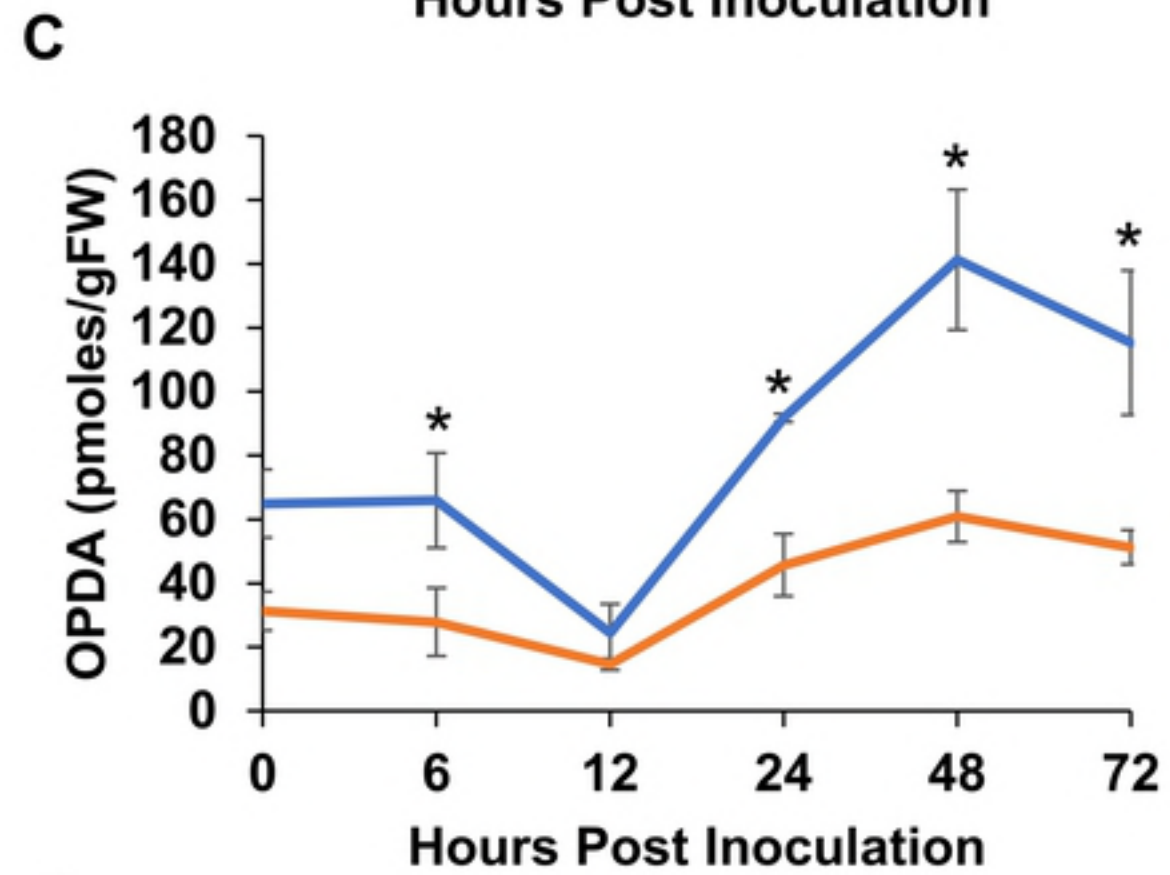

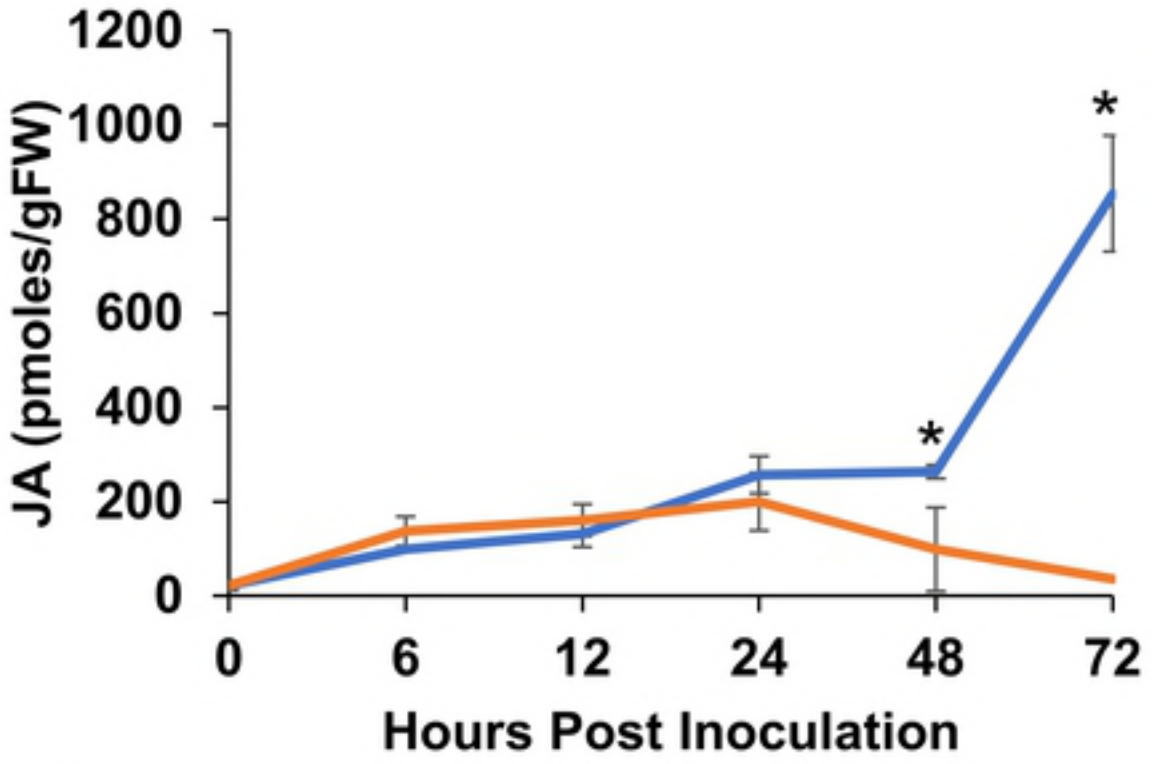

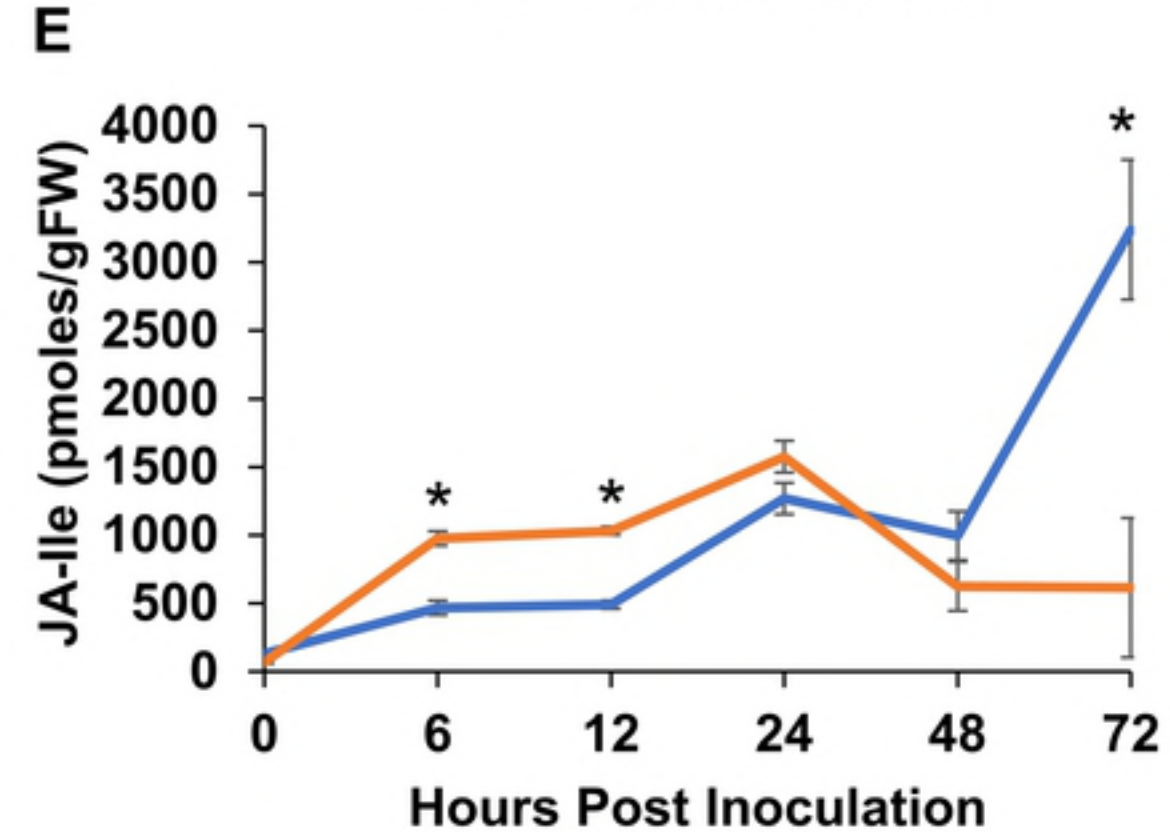

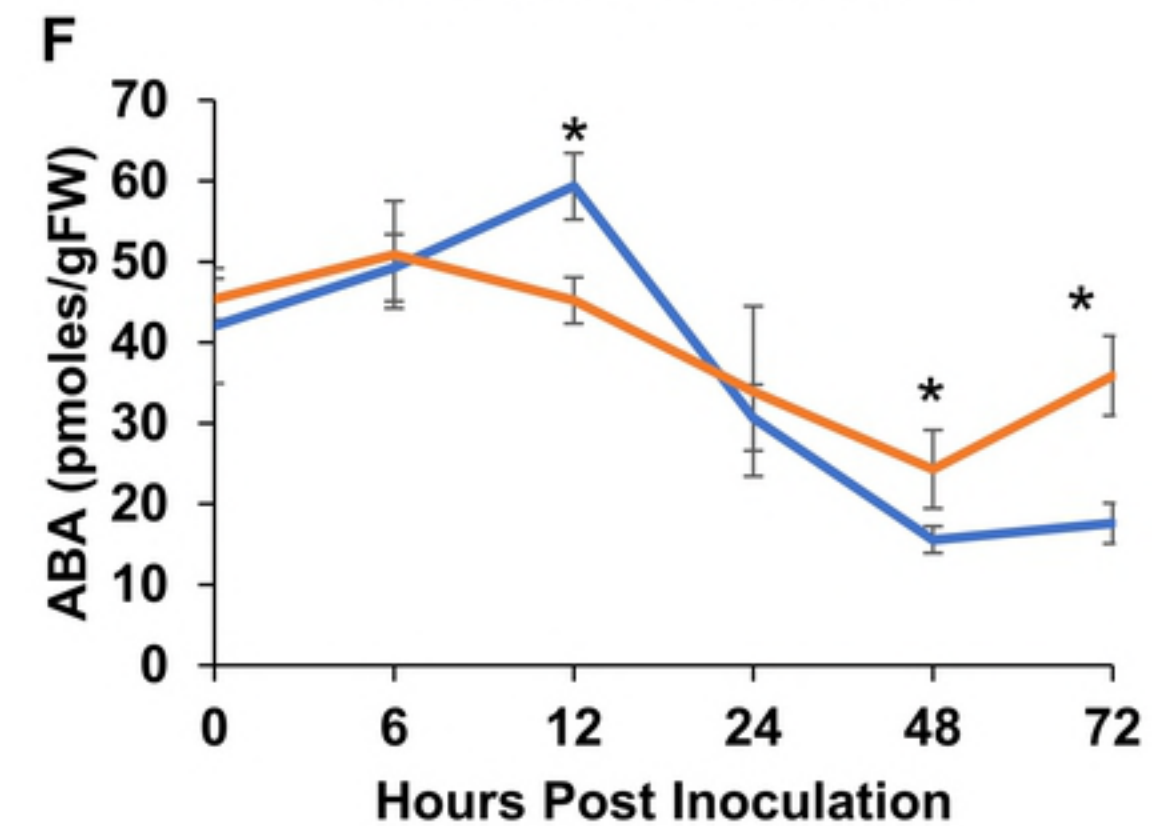

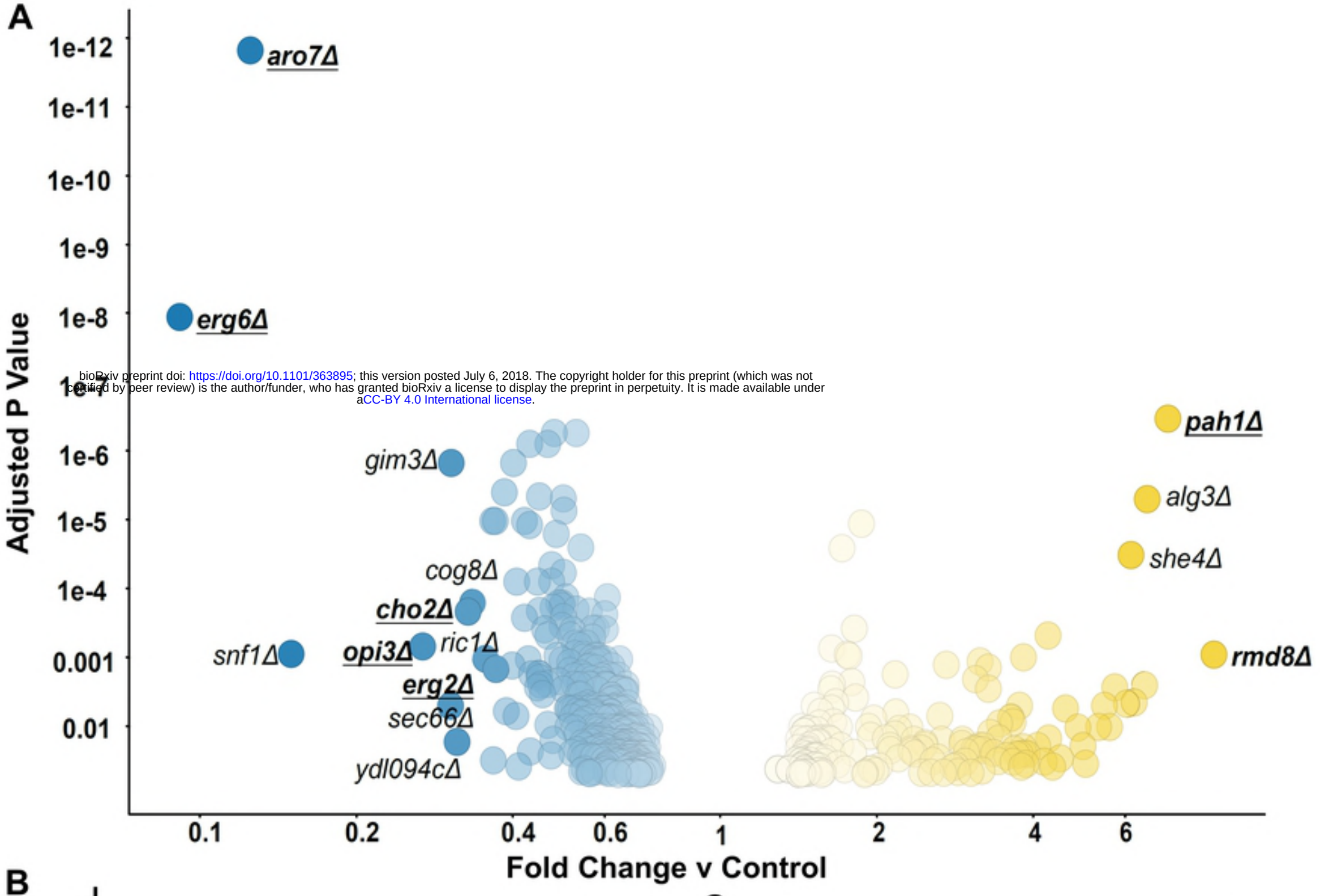

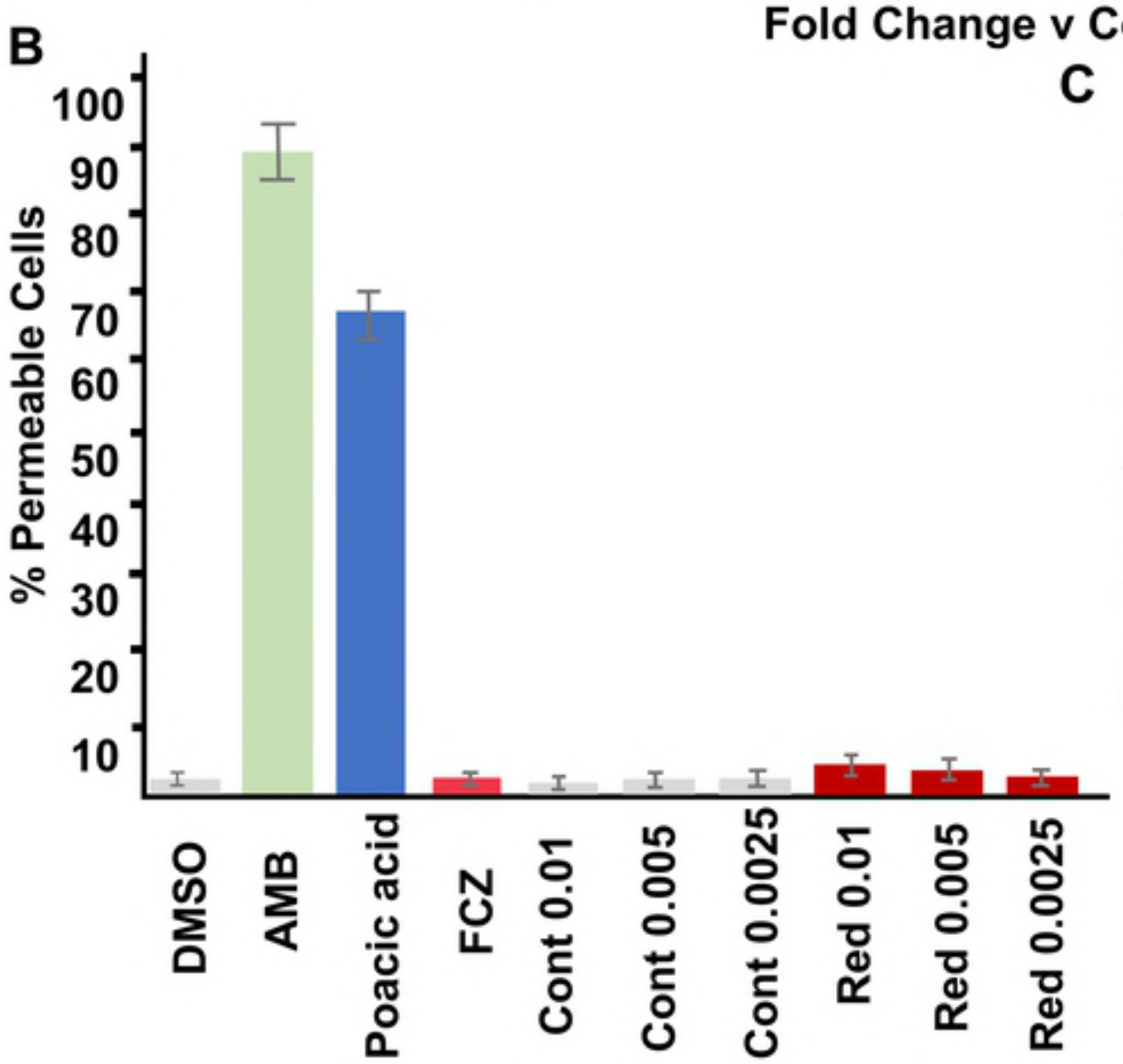

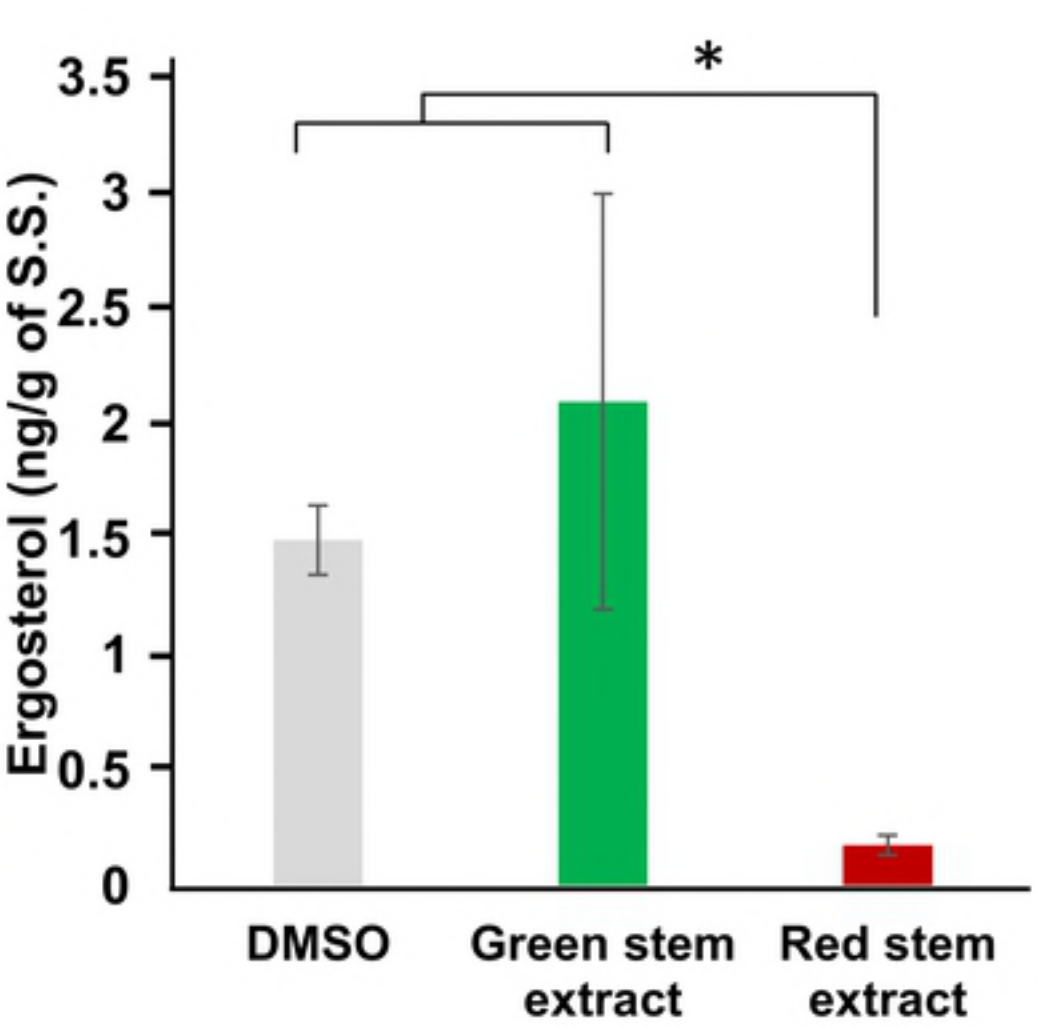

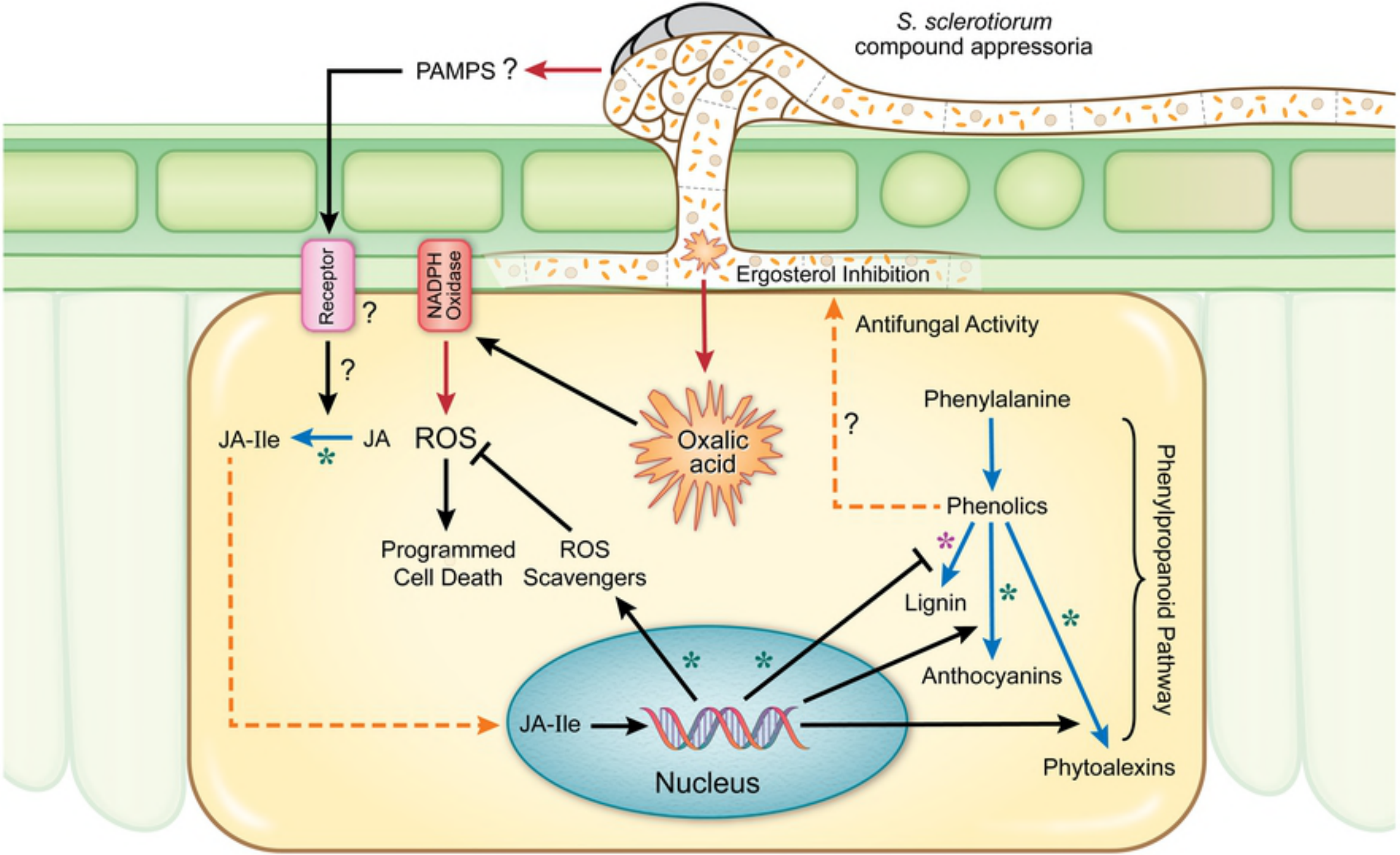
S. sclerotiorum
compound appressoria
PAMPS ?
Receptor
?
NADPH Oxidase
Ergosterol Inhibition
Antifungal Activity
?
?
JA-Ile
JA
ROS
Oxalic acid
Phenylalanine
Phenolics
Programmed Cell Death
ROS Scavengers
Lignin
Anthocyanins
Phenylpropanoid Pathway
JA-Ile
Nucleus
Phytoalexins